

TOWARD A TOPOLOGICAL ISO-STRING THEORY IN 4D ISO-DUAL SPACE-TIME: HYPOTHESIS AND PRELIMINARY CONSTRUCTION

Nathan O. Schmidt
Department of Mathematics
Boise State University
1910 University Drive
Boise, ID 83725, USA
nathanschmidt@u.boisestate.edu

November 2, 2013

Abstract

We propose a *preliminary* framework that engages iso-triplex numbers and deformation order parameters to encode the spatial states of Iso Open Topological Strings (Iso-OTS) for fermions and the temporal states of Iso Closed Topological Strings (Iso-CTS) for bosons, where space and time are iso-dual. The objective is to introduce an elementary Topological Iso-String Theory (TIST) that complies with the holographic principle and fundamentally represents the twisting, winding, and deforming of helical, spiral, and vortical information structures—*by default*—for attacking superfluidic motion patterns and energy states with iso-topic lifting. In general, these preliminary results indicate a cutting-edge, flexible, consistent, and powerful iso-mathematical framework with considerable representational capability that warrants further examination, collaboration, construction, and discipline.

Keywords: Holographic principle; Inopin holographic ring; Santilli iso-number; String model; Topological iso-string model; Fibonacci; Non-linear dynamics; Topological deformation.

1 Introduction

String theory is an active research framework in particle physics that aims to unify quantum mechanics and general relativity [1, 2]. The theory posits that the elementary particle states and interactions of our universe can be encoded as 1D oscillating lines, namely *strings* [1, 2]. In short, everything is theoretically well-defined in terms of vibrations and harmonics [1, 2]—a powerful, elegant, and beautiful idea [3]. In one context, string theory has evolved to be *conceptually* straightforward because today there are *two* general types of strings: open and closed [3, 4]. A *closed string* is a string that has no end-points, and therefore is topologically equivalent to a circle [3, 4]. Whereas an *open string*, on the other hand, has two end-points, and is therefore topologically equivalent to a line interval [3, 4]. Interactions between open strings can always result in closed strings [4]. Unfortunately, the existing mathematical framework that is designed to encode the string states is remarkably complex because it operates within 11D space-time [3]; so it cannot be directly verified in laboratory experiments and therefore, cannot withstand the heat of rigorous scientific scrutiny [5, 6]. Moreover, some argue that string theory is not even science [6, 7, 8].

It is known that helices, spirals, and vortices are *non-linear structures* that are *fundamental* to nature. For example, helical patterns are present in biological structures such as DNA and amino-acid sequences [9, 10, 11, 12, 13, 14, 15], while spiral and vortical patterns are inherent to super-current [16, 17], Bose-Einstein condensates [18, 19, 20], tornadoes [21, 22, 23], cyclones [24, 25, 26], and large-scale configurations such as galaxies and super-massive black holes [27, 28, 29, 30, 31]. The imperative need for this mode of non-linear architecture is furthermore exemplified by the topology twisting of Inopin [32], the hubius helix of Hu [33], and the helical strings of Tordova [34, 35]. Thus, given that string theory has been proposed for grand unification [1, 2, 3, 4], the said observations seem to indicate that, at minimum, an acceptable string-based unification candidate must be able to encode the energy and resonance state space of these non-linear structures so its interactional representation and predictive capability can be experimentally tested in a 4D space-time laboratory. So *why* does modern string theory fail to meet this critical scientific requirement? In particular, *what* is the underlying mechanistic assertion in the theory's conceptual and mathemat-

ical framework that generates this need for 11D complexity? *How* does this mysterious contention render the theory inapplicable to the laboratory?

In this preliminary paper, we launch an assault against the said inconsistencies of conventional string theory [5, 7, 8]: we begin to apply Santilli's iso-numbers [36, 37, 38, 39, 40, 41] and Inopin's holographic ring (IHR) topology [42, 43, 44] to initiate the construction of new *iso-strings* with isotriple numbers in the iso-dual 4D space-time of [45]. For this, the IHR encodes the dimension of time, which is an iso-metrically embedded topological sphere equipped with deformation order parameters that acquires a Berry phase and is simultaneously dual to two spatial 3-branes [42, 43, 44, 45] for iso-topic lifting [36, 37, 38, 39, 40, 41]. Here, the objective is to initiate the construction of an elementary TIST that complies with the holographic principle and fundamentally encodes the twisting, winding, and deforming of the helical, spiral, and vortical structures in nature. Therefore, the first step is to state our hypothesis: *using iso-numbers [36, 37, 38, 39, 40, 41, 45] and the IHR topology [42, 43, 44, 45], it may be possible to assemble a TIST that encodes helical, spiral, and vortical structures by default (with topological deformation order parameters for winding and twisting) to reduce the complexity of conventional string theory from 11D to 4D so it can be experimentally verified in the laboratory.* In other words, we argue that if these non-linear topological structures and iso-topic liftings are not built into the theory from the beginning, then the string's energy and resonance state space will inevitably become overly complicated because the underlying mathematical framework and encoding methodology is not designed to specifically handle the abundance of helical, spiral, and vortical features of nature. This hypothetically implies that conventional string theory implementations may be ill-equipped to deal with these non-linear scenarios simply because they lack the proper topological platform (with built-in winding and twisting). Thus, if one attempts to deploy 1D oscillating lines and circles to represent, for example, the above listed non-linear patterns in nature, one will *immediately* encounter *convolution* because the framework does not naturally account for the inherent and continual topological twisting, winding, deforming, and lifting properties from-the-start. Hence, when facing the "unification beast" with a string-based attack, we are inevitably confronted with the *illusion* of extreme representational complexity

that exceeds 4D space-time by multiple magnitude orders (i.e. 11D space-time) because it is inherently difficult to encode, for example, a vortex with a 1D oscillating line and/or circle, due to their structural limitations (i.e. they do not support topological twisting, winding, deforming, and lifting by default). To date, the coordinated assault on such monolithic creatures has resulted in an 11D space-time framework because, historically, string theorists have deemed it necessary to include additional degrees of freedom too sufficiently encode the (twisting, winding, and deforming) state space. Thus, it is difficult (if not impossible) to experimentally verify an 11D string theory in a conventional 4D space-time laboratory. As a result, string theory remains a highly controversial research framework and faces substantial opposition [5, 7, 8].

Therefore, our attack aims to support the conventional string theory approach [1, 2, 3, 4] by identifying a 4D TIST that circumvents the acknowledged 11D string theory complexity and limitations [5, 7, 8]. In particular, we will demonstrate that the preliminary 4D TIST approach that accounts for the twisting, winding, and deforming of natural structures by default is achieved by:

1. upgrading the conventional open string and closed string models in 11D space-time [1, 2, 3, 4] with OTS and CTS models built from triplex numbers in the dual 4D space-time IHR topology [42, 43, 44]; and
2. further upgrading the OTS and CTS models in the dual 4D space-time IHR topology [42, 43, 44] by iso-topically lifting [36, 37, 38, 39, 40, 41] them to Iso-OTS and Iso-CTS models built with iso-triplex numbers in the iso-dual 4D space-time IHR topology [45].

We prepare for our exploration with Section 2, where we initialize the dual 4D space-time IHR topology [42, 43, 44] locations for a quark-antiquark pair that will be represented with an OTS and CTS. Next, we launch with Section 3, where we introduce, define, and assemble a *preliminary* OTS, which comprises two topological components for encoding the spatial fermionic states: a *thin flux tube* and a circulating *super-current vortex*. For this, we provide one brief example on how the Fibonacci sequence may be

applied to interpret energy and resonance states of the OTS. Subsequently, in Section 4, we introduce, define, and assemble a *preliminary* CTS, which comprises two topological components for encoding the temporal bosonic states: the *IHR* [42, 43, 44, 45] and a circulating *helix*. Afterwards, in Section ??, we iso-topically lift the dual 4D space-time IHR topology, OTS, and CTS to define an iso-dual 4D space-time IHR topology, Iso-OTS, and Iso-CTS, respectively. Finally, we terminate our investigation with the brief discussion of Section 6, where we recapitulate our hypothesis, procedure, and results, and suggest future modes of research.

2 Initializing the quark-antiquark pair and its antisymmetric wavefunction

Here, we prepare for the initial topological string theory definitions by using the work of [42, 43, 44, 45] to encode the triplex locations for the quark-antiquark pair in the dual 4D space-time IHR topology.

Let X be the set of complex numbers and *2D Position-Point State Space* (2D-PPSS) for the dual 3D space-time IHR topology, which is embedded in the set of triplex numbers and *3D Position-Point State Space* (3D-PPSS) Y for the dual 4D space-time IHR topology, such that $X \subset Y$ [42, 43, 44, 45]—see Figure 1. The T^1 of eq. (16) in [45] is the *1-sphere IHR* that is isometrically embedded in both X and Y because $T^1 \subset X$ and $T^1 \subset Y$ [42, 43, 44, 45], such that T^1 is the great circle of the *2-sphere IHR* $T^2 \subset Y$ of eq. (33) in [45], where both T^1 and T^2 have the amplitude-radius ϵ . Here, we will simultaneously initialize a quark-antiquark pair that is confined to both T^1 and T^2 . Thus, a complex number and *2D Position-Point State* (2D-PPS) $\vec{x} \in X$ is defined in eq. (6) of [45] as

$$x = \vec{x} = \vec{x}_{\mathbb{R}} + \vec{x}_{\mathbb{I}} = (\vec{x}) = (|\vec{x}|, \langle \vec{x} \rangle)_P = (\vec{x}_{\mathbb{R}}, \vec{x}_{\mathbb{I}})_C, \quad \forall \vec{x} \in X, \quad (1)$$

where \vec{x} is a *dual 2D Cartesian-polar coordinate-vector state*, such that $(\vec{x}) = (|\vec{x}|, \langle \vec{x} \rangle)_P$ is the 2D polar coordinate-vector state and $(\vec{x}_{\mathbb{R}}, \vec{x}_{\mathbb{I}})_C$ is the 2D Cartesian coordinate-vector state [45]. Moreover, given that $X \subset Y$, the $\vec{x} \in X$ of eq. (1) simultaneously refers to a triplex number and *3D Position-Point State* (3D-PPS) $\vec{y} \in Y$ because $\vec{x}_{\mathbb{R}} = \vec{y}_{\mathbb{R}}$ and $\vec{x}_{\mathbb{I}} = \vec{y}_{\mathbb{I}}$, which is defined in eq. (17) of [45] as

$$y = \vec{y} = \vec{y}_{\mathbb{R}} + \vec{y}_{\mathbb{I}} + \vec{y}_Z = (\vec{y}) = (|\vec{y}|, \langle \vec{y} \rangle, [\vec{y}])_S = (\vec{y}_{\mathbb{R}}, \vec{y}_{\mathbb{I}}, \vec{y}_Z)_C, \quad \forall \vec{y} \in Y, \quad (2)$$

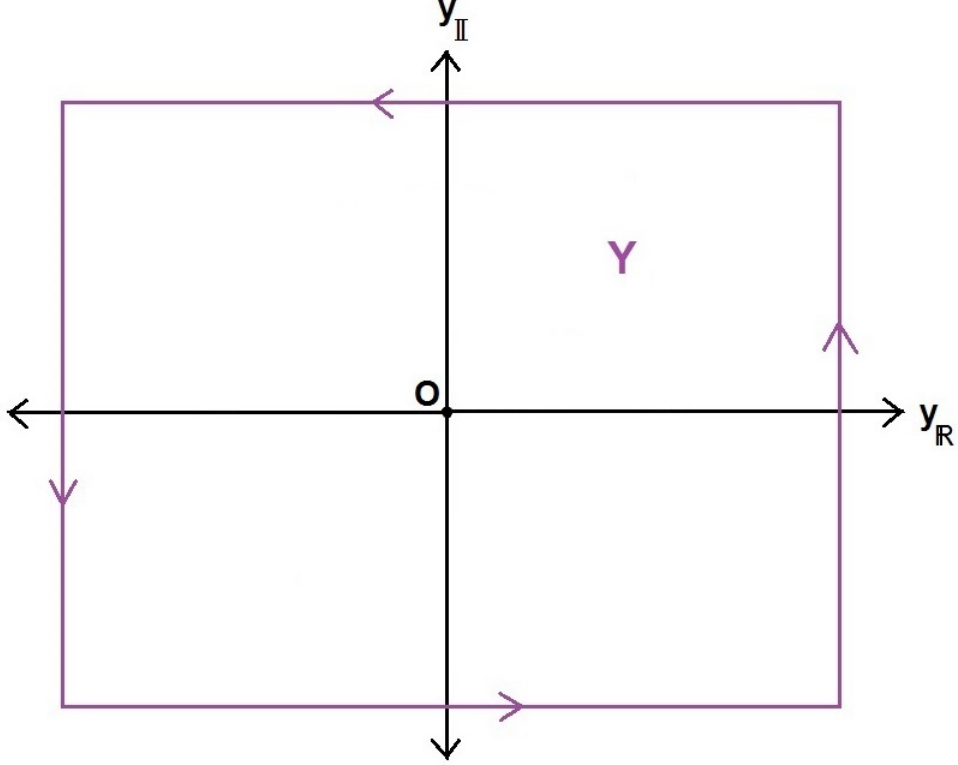


Fig. 1: The 2D-PPSS X is embedded in the 3D-PPSS Y , so $X \subset Y$, such that X and Y share the same $y_{\mathbb{R}}$ -axis and $y_{\mathbb{I}}$ -axis, but Y contains the additional $y_{\mathbb{Z}}$ -axis [43, 44, 45].

where \vec{y} is a *dual 3D Cartesian-polar coordinate-vector state*, such that $(|\vec{y}|, \langle \vec{y} \rangle, [\vec{y}])_S$ is the 3D spherical (extended polar) coordinate-vector state and $(\vec{y}_{\mathbb{R}}, \vec{y}_{\mathbb{I}}, \vec{y}_{\mathbb{Z}})_C$ is the 3D Cartesian coordinate-vector state [45].

We let q be a quark, namely a *non-Abelian color-electric-magnetic quark monopole* from [42], where eq. (35) in [43] defines q 's 3D-PPS $\vec{q} \in T^1 \subset T^2 \subset Y$ as

$$q : \vec{q} \equiv \vec{q}_{\mathbb{R}} + \vec{q}_{\mathbb{I}} + \vec{q}_{\mathbb{Z}} = (\vec{q}) = (|\vec{q}|, \langle \vec{q} \rangle, [\vec{q}])_S = (\vec{q}_{\mathbb{R}}, \vec{q}_{\mathbb{I}}, \vec{q}_{\mathbb{Z}})_C. \quad (3)$$

Next, we let \bar{q} be the antiquark that is the antiparticle of q , namely a *non-Abelian anticolor-electric-magnetic antiquark antimonopole* from [42], where

eq. (35) in [43] similarly defines \vec{q} 's 3D-PPS $\vec{q} \in T^1 \subset T^2 \subset Y$ as

$$\vec{q} : \vec{q} \equiv \vec{q}_{\mathbb{R}} + \vec{q}_{\mathbb{I}} + \vec{q}_Z = (\vec{q}) = (|\vec{q}|, \langle \vec{q} \rangle, [\vec{q}])_S = (\vec{q}_{\mathbb{R}}, \vec{q}_{\mathbb{I}}, \vec{q}_Z)_C. \quad (4)$$

The pair $q\bar{q}$ represents a *color-electric-magnetic dipole* [42]. For eqs. (3–4), the quark-antiquark 3D-PPS antisymmetric location duality constraints of eqs. (72–73) in [43] are written for the $q\bar{q}$ pair as

$$\begin{aligned} \vec{q}_{\mathbb{R}} + \vec{q}_{\mathbb{I}} + \vec{q}_Z &= -\vec{q}_{\mathbb{R}} - \vec{q}_{\mathbb{I}} - \vec{q}_Z \\ |\vec{q}| &= |\vec{\bar{q}}| \\ \langle \vec{q} \rangle &= \langle \vec{\bar{q}} \rangle \pm \pi \\ [\vec{q}] &= [\vec{\bar{q}}] \pm \pi \\ \vec{q}_{\mathbb{R}} &= -\vec{\bar{q}}_{\mathbb{R}} \\ \vec{q}_{\mathbb{I}} &= -\vec{\bar{q}}_{\mathbb{I}} \\ \vec{q}_Z &= -\vec{\bar{q}}_Z, \end{aligned} \quad (5)$$

where the encoded $q\bar{q}$ states adhere to the uniformly-arranged “phase-OPS and inclination-OPS antiferromagnetic ordering constraints” of eq. (74) in [43]

$$\begin{aligned} \langle \vec{\psi}_J(\vec{q}) \rangle &= \langle \vec{\psi}_J(\vec{\bar{q}}) \rangle \pm \pi \\ [\vec{\psi}_J(\vec{q})] &= [\vec{\psi}_J(\vec{\bar{q}})] \pm \pi \end{aligned} \quad (6)$$

for $|\vec{\psi}_J(\vec{q})| = |\vec{\psi}_J(\vec{\bar{q}})|$ with Rashba spin-orbit coupling [46]. Eq. (6) is significant because it employs the Rashba spin-orbit coupling [46] to correlate the magnetic 3D-OPSs and thereby simplify the overall 3D representation of the antisymmetric wavefunction [42, 43]. Therefore, eqs. (3–6) satisfy the relevant 3D wavefunction states of eqs. (75–83) in [43] and the 3D CPT-theorem implementation of eqs. (84–86) in [43]. Hence, $\vec{q}, \vec{\bar{q}} \in T^1 \subset T^2 \subset Y$ are equidistant from the origin-point $O \in Y_-$ of [43], such that the amplitude-radius of T^1 and T^2 is

$$\epsilon = |\vec{q}| = |\vec{\bar{q}}|, \quad (7)$$

where the 3D Cartesian distance for $q\bar{q}$'s geometrical line segment $\overline{q\bar{q}}$ is defined as

$$d(\vec{q}, \vec{\bar{q}}) = d_{q\bar{q}} = \sqrt{(\vec{q}_{\mathbb{R}} - \vec{\bar{q}}_{\mathbb{R}})^2 + (\vec{q}_{\mathbb{I}} - \vec{\bar{q}}_{\mathbb{I}})^2 + (\vec{q}_Z - \vec{\bar{q}}_Z)^2} = |\vec{q}| + |\vec{\bar{q}}|, \quad (8)$$

so $O \in Y_-$ is the “mid 3D-PPS” of $\overline{q\bar{q}}$.

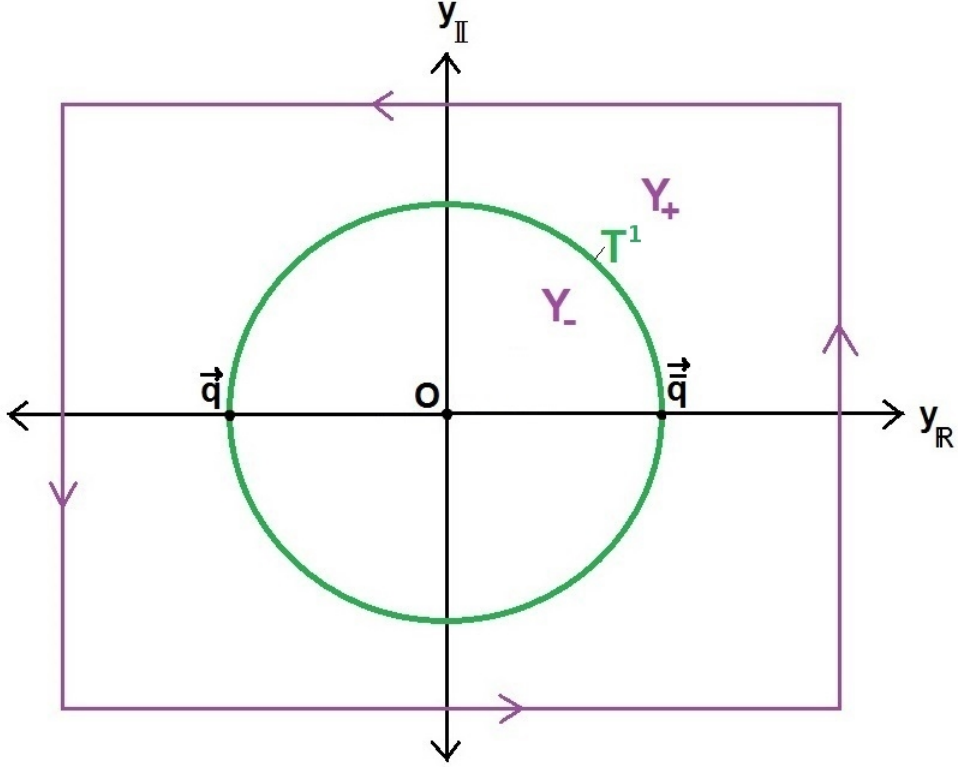


Fig. 2: The $q\bar{q}$ dipole is confined to T^1 (the great circle of T^2) in the dual 4D space-time IHR topology [42, 43, 44, 45].

At this point, we've initialized the 3D-PPSS and 3D-OPSS for the $q\bar{q}$ dipole that is confined to the IHR T^1 —see Figure 2—so we are ready to proceed with the topological string construction.

3 Open topological strings for fermion spatial states

Here, we introduce, define, and assemble an OTS and its spatial states for the fermion features of the $q\bar{q}$ dipole confined to T^1 using the triplex encoding framework of [43, 44, 45]. In general, the OTS contains two distinct information sub-structures: the

1. *Open Topological String Thin Flux Tube* (OTS-Tube), a *linear* infor-

mation sub-structure; and

2. *Open Topological String Super-Current Vortex* (OTS-Vortex), a *non-linear* information sub-structure.

Here, we identify, construct, and discuss both OTS sub-structures and their interdependence.

3.1 Open topological string flux tubes

The OTS-Tube for the $q\bar{q}$ dipole is defined as a *topological 1D line interval space of 3D-PPSs in a 3D-PPSS sub-space*, namely

$$\begin{aligned} \bar{S}_{\vec{q}, \vec{q}} \subset Y_- &\equiv \bar{S}(\vec{q}, \vec{q}) \subset Y_- \equiv \{\vec{y} \in Y_- : \vec{y} \in \overline{\vec{q}, \vec{q}}\} \\ &\equiv \{\vec{y} \in Y_- : 0 < |\vec{y}| < |\epsilon|, \langle \vec{y} \rangle = \langle \vec{q} \rangle, [\vec{y}] = [\vec{q}]\} \cup \{O\} \cup \\ &\quad \{\vec{y} \in Y_- : 0 < |\vec{y}| < |\epsilon|, \langle \vec{y} \rangle = \langle \vec{q} \rangle, [\vec{y}] = [\vec{q}]\} \end{aligned} \quad (9)$$

which is the *ordered continuous 3D-PPS set* and *3D-PPS sub-surface* for the interval (\vec{q}, \vec{q}) along the 1D line segment set $\overline{\vec{q}, \vec{q}}$, where the order of the particle arguments \vec{q} and \vec{q} determine the order of $\bar{S}_{\vec{q}, \vec{q}}$. Note that $\bar{S}_{\vec{q}, \vec{q}}$ does not actually include the 3D-PPSs \vec{q} and \vec{q} , but it is said to encode $q\bar{q}$ dipole spatial states (in subsequent sections, we will show why this exclusion and representation is meaningful).

Now, due to the fact that Y_- and $\overline{\vec{q}, \vec{q}}$ are both continuous, and because $\bar{S}_{\vec{q}, \vec{q}}$ is a 3D-PPS sub-space of Y_- , then the *OTS-Tube 3D-PPS cardinality* is expressed as

$$|\bar{S}_{\vec{q}, \vec{q}}| \equiv |\bar{S}(\vec{q}, \vec{q})| \equiv \infty \quad (10)$$

for an *infinite* number of 3D-PPSs within $\bar{S}_{\vec{q}, \vec{q}}$, even though the *OTS-Tube 3D-PPS length* is expressed as

$$||\bar{S}_{\vec{q}, \vec{q}}|| \equiv ||\bar{S}(\vec{q}, \vec{q})|| \equiv d_{q\bar{q}} \quad (11)$$

for the *finite* 3D Cartesian distance of eq. (8), which includes $\vec{q}, \vec{q} \in T^1$ as well. The cardinality $|\bar{S}_{\vec{q}, \vec{q}}|$ of eq. (10) is infinite because it is continuous and smooth sub-space of mathematical objects. From this, it is evident that

$O \in Y_-$ is the mid 3D-PPS of $\bar{S}_{\vec{q}, \vec{q}}$, so we split $\bar{S}_{\vec{q}, \vec{q}}$ into the *dual OTS-Tube 3D-PPS sub-spaces*

$$\begin{aligned} \bar{S}_{O, \vec{q}} \subset \bar{S}_{\vec{q}, \vec{q}} &\equiv \bar{S}(O, \vec{q}) \subset \bar{S}(\vec{q}, \vec{q}) \\ &\equiv \{\vec{y} \in \bar{S}(\vec{q}, \vec{q}) : 0 < |\vec{y}| < |\epsilon|, \langle \vec{y} \rangle = \langle \vec{q} \rangle, [\vec{y}] = [\vec{q}]\} \end{aligned} \quad (12)$$

for the “left-handed” or “quark-handed” OTS-Tube 3D-PPS sub-space, namely the *Quark-OTS-Tube*, and

$$\begin{aligned} \bar{S}_{O, \vec{q}} \subset \bar{S}_{\vec{q}, \vec{q}} &\equiv \bar{S}(O, \vec{q}) \subset \bar{S}(\vec{q}, \vec{q}) \\ &\equiv \{\vec{y} \in \bar{S}(\vec{q}, \vec{q}) : 0 < |\vec{y}| < |\epsilon|, \langle \vec{y} \rangle = \langle \vec{q} \rangle, [\vec{y}] = [\vec{q}]\} \end{aligned} \quad (13)$$

for the “right-handed” or “antiquark-handed” OTS-Tube 3D-PPS sub-space, namely the *Antiquark-OTS-Tube*, of the ordered 3D-PPS subset intervals (O, \vec{q}) and (O, \vec{q}) , respectively. For notational preference, we may opt to use

$$\bar{S}_{\vec{q}} \equiv \bar{S}_{O, \vec{q}} \equiv \bar{S}(O, \vec{q}) \quad (14)$$

$$\bar{S}_{\vec{q}} \equiv \bar{S}_{O, \vec{q}} \equiv \bar{S}(O, \vec{q}) \quad (15)$$

for simplicity. Thus, for the Quark-OTS-Tube and the Antiquark-OTS-Tube the infinite cardinalities are

$$|\bar{S}_{\vec{q}}| \equiv |\bar{S}_{\vec{q}}| \equiv \frac{1}{2} |\bar{S}_{\vec{q}, \vec{q}}| \equiv \infty \quad (16)$$

and the finite lengths are

$$\|\bar{S}_{\vec{q}}\| \equiv \|\bar{S}_{\vec{q}}\| \equiv \frac{1}{2} \|\bar{S}_{\vec{q}, \vec{q}}\| \equiv \frac{1}{2} d_{q\bar{q}}. \quad (17)$$

Hence, we recapitulate that

$$\begin{aligned} \bar{S}_{\vec{q}} \cup \{O\} \cup \bar{S}_{\vec{q}} &\equiv \bar{S}_{\vec{q}, \vec{q}} \\ \bar{S}_{\vec{q}} \cap \{O\} \cap \bar{S}_{\vec{q}} &\equiv \emptyset \end{aligned} \quad (18)$$

and

$$\begin{aligned} \bar{S}[0, \vec{q}] \cup \bar{S}[0, \vec{q}] &\equiv \bar{S}[\vec{q}, \vec{q}] \equiv \{\vec{q}\} \cup \bar{S}_{\vec{q}, \vec{q}} \cup \{\vec{q}\} \\ \bar{S}[0, \vec{q}] \cap \bar{S}[0, \vec{q}] &\equiv \{O\} \\ \bar{S}(0, \vec{q}) \cap \bar{S}(0, \vec{q}) &\equiv \emptyset. \end{aligned} \quad (19)$$

Therefore, because of the quark-antiquark duality and baryon-antibaryon duality of [42, 43], the Quark-OTS-Tube and the Antiquark-OTS-Tube are also dual, so we express the *OTS-Tube 3D-PPS duality functions*

$$\begin{aligned} h_{\bar{q} \rightarrow \bar{q}}(\bar{S}) : \bar{S}_{\bar{q}} &\rightarrow \bar{S}_{\bar{q}} \\ h_{\bar{q} \rightarrow \bar{q}}(\bar{S}) : \bar{S}_{\bar{q}} &\rightarrow \bar{S}_{\bar{q}}. \end{aligned} \quad (20)$$

Thus, to further exemplify the duality of eq. (20), we utilize the similarity of eq. (5) to apply the 3D-PPS antisymmetric location duality constraints of eqs. (72–73) in [43] to $\bar{S}_{\bar{q}, \bar{q}}$ to establish the *OTS-Tube 3D-PPS antisymmetric duality constraints*

$$\begin{aligned} \vec{y}_{\mathbb{R}} + \vec{y}_{\mathbb{I}} + \vec{y}_{\mathbb{Z}} &= -\vec{y}_{\mathbb{R}} - \vec{y}_{\mathbb{I}} - \vec{y}_{\mathbb{Z}} \\ |\vec{y}| &= |\vec{y}| \\ \langle \vec{y} \rangle &= \langle \vec{y} \rangle \pm \pi \\ [\vec{y}] &= [\vec{y}] \pm \pi \\ \vec{y}_{\mathbb{R}} &= -\vec{y}_{\mathbb{R}} \\ \vec{y}_{\mathbb{I}} &= -\vec{y}_{\mathbb{I}} \\ \vec{y}_{\mathbb{Z}} &= -\vec{y}_{\mathbb{Z}}, \end{aligned} \quad (21)$$

$\forall \vec{y} \in \bar{S}_{\bar{q}}, \forall \vec{y} \in \bar{S}_{\bar{q}}$, for the 3D-PPS parity-symmetry constraint of eq. (85) in [43].

At this point, we've introduced, defined, and assembled the OTS-Tube $\bar{S}_{\bar{q}, \bar{q}}$ for the $q\bar{q}$ dipole in Y that is confined to T^1 , where $\bar{S}_{\bar{q}, \bar{q}}$ comprises the Quark-OTS-Tube $\bar{S}_{\bar{q}}$ and Antiquark-OTS-Tube $\bar{S}_{\bar{q}}$, which are dual, inverse, opposite, and reverse topological sub-structures that are interdependent—all of this is consistent with the quark confinement topology and baryon-antibaryon duality of [42, 43].

3.2 Open topological string super-current vortices

Here, we assemble the OTS-Vortex for the $q\bar{q}$ dipole by equipping the OTS-Tube $\bar{S}_{\bar{q}, \bar{q}}$ with a 3D-OPS layer of fractional statistics for the “generic” topological deformations of [43], which upgrades the framework of [42]. In fact, as we will show, the OTS-Vortex actually comprises dual OTS-Vortices that correspond to the Quark-OTS-Tube $\bar{S}_{\bar{q}}$ and Antiquark-OTS-Tube $\bar{S}_{\bar{q}}$.

Now, from eq. (50) in [43] we know that Y can be assigned a 3D-OPS layer for topological deformations. Thus, because $\bar{S}_{\vec{q},\vec{q}} \subset Y$, we know that eq. (50) in [43] applies to $\bar{S}_{\vec{q},\vec{q}}$. Hence, the first step is to define the *topological 1D line interval space of 3D-OPSs* to $\bar{S}_{\vec{q},\vec{q}}$ as

$$\vec{S}_{\vec{q},\vec{q}} \equiv \vec{S}(\vec{q},\vec{q}) \equiv \bigcup_{\vec{y} \in \bar{S}(\vec{q},\vec{q})} \vec{\psi}_{\rightarrow}(\vec{y}), \quad (22)$$

which assigns $\bar{S}_{\vec{q},\vec{q}}$'s 3D-OPS layer for topological deformations, where $\vec{\psi}_{\rightarrow}(\vec{y})$ is the 3D-OPS in the 3D-OPSS $\vec{\Phi}_{\rightarrow}(\vec{y})$ at \vec{y} , such that $\vec{\psi}_{\rightarrow}(\vec{y}) \in \vec{\Phi}_{\rightarrow}(\vec{y})$; $\vec{S}_{\vec{q},\vec{q}}$ of eq. (22) is called the *OTS-Vortex Foundation*, which is a continuous ordered 3D-OPS set, such that $\vec{S}_{\vec{q},\vec{q}}$'s infinite cardinality is

$$|\vec{S}_{\vec{q},\vec{q}}| \equiv |\bar{S}_{\vec{q},\vec{q}}| \equiv \infty, \quad (23)$$

and $\vec{S}_{\vec{q},\vec{q}}$'s finite length is

$$\|\vec{S}_{\vec{q},\vec{q}}\| \equiv \|\bar{S}_{\vec{q},\vec{q}}\| \equiv d_{q\bar{q}}. \quad (24)$$

The cardinalities and lengths of eqs. (23–24) are dual and equivalent because each 3D-PPS of $\bar{S}_{\vec{q},\vec{q}}$ is assigned a corresponding 3D-OPS in $\vec{S}_{\vec{q},\vec{q}}$ to encode a physical deformation. Figure 3 depicts a 3D-OPS layer assignment to the OTS-Tube $\bar{S}_{\vec{q},\vec{q}}$ for topological deformations; this method is used to build the OTS-Vortex Foundation $\vec{S}_{\vec{q},\vec{q}}$.

Therefore, the 3D-PPSs of $\bar{S}_{\vec{q},\vec{q}}$ and the corresponding 3D-OPSs of $\vec{S}_{\vec{q},\vec{q}}$ are sequentially summed to define the OTS-Vortex for the $q\bar{q}$ dipole, which is a *topological 3D vortex space of 3D-OPSs*, as

$$\tilde{S}_{\vec{q},\vec{q}} \subset Y_- \equiv \tilde{S}(\vec{q},\vec{q}) \subset Y_- \equiv \bigcup_{\vec{y} \in \bar{S}_{\vec{q},\vec{q}}} \vec{y} + \vec{\psi}_{\rightarrow}(\vec{y}) \equiv \bigcup_{\vec{y} \in \bar{S}_{\vec{q},\vec{q}}} \gamma(\vec{y}), \quad (25)$$

where

$$\vec{\gamma} \equiv \gamma(\vec{y}) \equiv \vec{y} + \vec{\psi}_{\rightarrow}(\vec{y}), \quad \forall \vec{y} \in \bar{S}_{\vec{q},\vec{q}}, \quad \forall \vec{\psi}_{\rightarrow}(\vec{y}) \in \vec{S}_{\vec{q},\vec{q}}, \quad (26)$$

such that $\vec{\gamma} \subset \tilde{S}_{\vec{q},\vec{q}} \subset Y_-$. At this point, we do not know the exact structure, shape, or length of $\tilde{S}_{\vec{q},\vec{q}}$ because it depends on a number of features (that

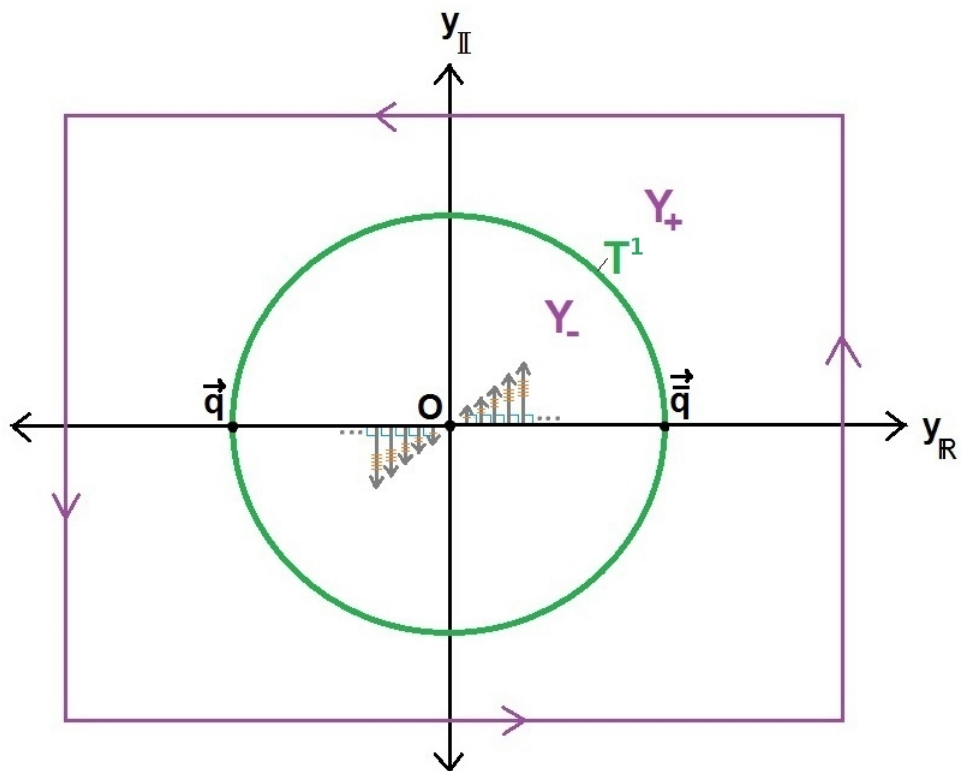


Fig. 3: A 3D-OPS layer is assigned to the interval (\vec{q}, \vec{q}) along the 1D line segment set \vec{q}, \vec{q} , which will become the OTS-Tube $\vec{S}_{\vec{q}, \vec{q}}$ with topological deformations that form the OTS-Vortex Foundation $\vec{S}_{\vec{q}, \vec{q}}$ for the OTS-Vortex $\vec{S}_{\vec{q}, \vec{q}}$.

we will soon discuss), but we do know that it must somehow wind around $\vec{S}_{\vec{q},\vec{q}}$, has some finite length $||\vec{S}_{\vec{q},\vec{q}}||$, such that $||\vec{S}_{\vec{q},\vec{q}}|| > d_{q\bar{q}}$, and bares an infinite cardinality $|\vec{S}_{\vec{q},\vec{q}}| \equiv \infty$ —for now, these preliminary and approximate constraints are all that we need to be aware of.

Next, we split the OTS-Vortex Foundation $\vec{S}_{\vec{q},\vec{q}}$ into dual sub-structures, just as we did with $\vec{S}_{\vec{q},\vec{q}}$ in the previous section, to ultimately demonstrate that they are inverses, opposites, and reverses for compliance with [42, 43]. Thus, we split $\vec{S}_{\vec{q},\vec{q}}$ into the *dual OTS-Vortex Foundation 3D-OPS sub-spaces*

$$\vec{S}_{O,\vec{q}} \subset \vec{S}_{\vec{q},\vec{q}} \equiv \vec{S}(O, \vec{q}) \subset \vec{S}(\vec{q}, \vec{q}) \equiv \bigcup_{\vec{y} \in \vec{S}_{O,\vec{q}}} \vec{\psi}_{\rightarrow}(\vec{y}) \quad (27)$$

for the left-handed or quark-handed OTS-Vortex Foundation 3D-OPS sub-space, namely the *Quark-OTS-Vortex Foundation*, and

$$\vec{S}_{O,\vec{q}} \subset \vec{S}_{\vec{q},\vec{q}} \equiv \vec{S}(O, \vec{q}) \subset \vec{S}(\vec{q}, \vec{q}) \equiv \bigcup_{\vec{y} \in \vec{S}_{O,\vec{q}}} \vec{\psi}_{\rightarrow}(\vec{y}) \quad (28)$$

for the right-handed or antiquark-handed OTS-Vortex Foundation 3D-OPS sub-space, namely the *Antiquark-OTS-Vortex Foundation*. Additionally, for notational preference, we may opt to use

$$\vec{S}_{\vec{q}} \equiv \vec{S}_{O,\vec{q}} \equiv \vec{S}(O, \vec{q}) \quad (29)$$

$$\vec{S}_{\vec{q}} \equiv \vec{S}_{O,\vec{q}} \equiv \vec{S}(O, \vec{q}) \quad (30)$$

for simplicity. Subsequently, we rewrite eq. (20) to express the *OTS-Vortex Foundation 3D-OPS duality functions*

$$h_{\vec{q} \rightarrow \vec{q}}(\vec{S}) : \vec{S}_{\vec{q}} \rightarrow \vec{S}_{\vec{q}} \quad (31)$$

$$h_{\vec{q} \rightarrow \vec{q}}(\vec{S}) : \vec{S}_{\vec{q}} \rightarrow \vec{S}_{\vec{q}},$$

for which eq. (21) is translated to define the *OTS-Vortex Foundation 3D-*

OPS antisymmetric duality constraints

$$\begin{aligned}
\vec{\psi}_{\rightarrow}(\vec{y})_{\mathbb{R}} + \vec{\psi}_{\rightarrow}(\vec{y})_{\mathbb{I}} + \vec{\psi}_{\rightarrow}(\vec{y})_Z &= -\vec{\psi}_{\rightarrow}(\vec{y})_{\mathbb{R}} - \vec{\psi}_{\rightarrow}(\vec{y})_{\mathbb{I}} - \vec{\psi}_{\rightarrow}(\vec{y})_Z \\
|\vec{\psi}_{\rightarrow}(\vec{y})| &= |\vec{\psi}_{\rightarrow}(\vec{y})| \\
\langle \vec{\psi}_{\rightarrow}(\vec{y}) \rangle &= \langle \vec{\psi}_{\rightarrow}(\vec{y}) \rangle \pm \pi \\
[\vec{\psi}_{\rightarrow}(\vec{y})] &= [\vec{\psi}_{\rightarrow}(\vec{y})] \pm \pi \\
\vec{\psi}_{\rightarrow}(\vec{y})_{\mathbb{R}} &= -\vec{\psi}_{\rightarrow}(\vec{y})_{\mathbb{R}} \\
\vec{\psi}_{\rightarrow}(\vec{y})_{\mathbb{I}} &= -\vec{\psi}_{\rightarrow}(\vec{y})_{\mathbb{I}} \\
\vec{\psi}_{\rightarrow}(\vec{y})_Z &= -\vec{\psi}_{\rightarrow}(\vec{y})_Z,
\end{aligned} \tag{32}$$

$$\forall \vec{\psi}_{\rightarrow}(\vec{y}) \in \vec{S}_{\vec{q}}, \forall \vec{\psi}_{\rightarrow}(\vec{y}) \in \vec{S}_{\vec{q}}.$$

Consequently, we split the OTS-Vortex $\tilde{S}_{\vec{q},\vec{q}}$ into dual sub-structures, just as we did with $\vec{S}_{\vec{q},\vec{q}}$ for compliance with [42, 43]. Thus, we split $\tilde{S}_{\vec{q},\vec{q}}$ into the *dual OTS-Vortex 3D-PPS sub-spaces*

$$\tilde{S}_{O,\vec{q}} \subset \tilde{S}_{\vec{q},\vec{q}} \equiv \tilde{S}(O, \vec{q}) \subset \tilde{S}(\vec{q}, \vec{q}) \equiv \bigcup_{\vec{y} \in \tilde{S}_{O,\vec{q}}} \vec{y} + \vec{\psi}_{\rightarrow}(\vec{y}) \equiv \bigcup_{\vec{y} \in \tilde{S}_{O,\vec{q}}} \gamma(\vec{y}) \tag{33}$$

for the left-handed or quark-handed OTS-Vortex 3D-PPS sub-space, namely the *Quark-OTS-Vortex*, and

$$\tilde{S}_{O,\vec{q}} \subset \tilde{S}_{\vec{q},\vec{q}} \equiv \tilde{S}(O, \vec{q}) \subset \tilde{S}(\vec{q}, \vec{q}) \equiv \bigcup_{\vec{y} \in \tilde{S}_{O,\vec{q}}} \vec{y} + \vec{\psi}_{\rightarrow}(\vec{y}) \equiv \bigcup_{\vec{y} \in \tilde{S}_{O,\vec{q}}} \gamma(\vec{y}) \tag{34}$$

for the right-handed or antiquark-handed OTS-Vortex 3D-PPS sub-space, namely the *Antiquark-OTS-Vortex*. Additionally, for notational preference, we may opt to use

$$\tilde{S}_{\vec{q}} \equiv \tilde{S}_{O,\vec{q}} \equiv \tilde{S}(O, \vec{q}) \tag{35}$$

$$\tilde{S}_{\vec{q}} \equiv \tilde{S}_{O,\vec{q}} \equiv \tilde{S}(O, \vec{q}) \tag{36}$$

for simplicity. Subsequently, we rewrite eq. (20) to express the *OTS-Vortex 3D-PPS duality functions*

$$h_{\vec{q} \rightarrow \vec{q}}(\tilde{S}) : \tilde{S}_{\vec{q}} \rightarrow \tilde{S}_{\vec{q}} \tag{37}$$

$$h_{\vec{q} \rightarrow \vec{q}}(\tilde{S}) : \tilde{S}_{\vec{q}} \rightarrow \tilde{S}_{\vec{q}},$$

for which eq. (21) applies to define the *OTS-Vortex 3D-PPS antisymmetric duality constraints*

$$\begin{aligned}
\vec{\gamma}_{\mathbb{R}} + \vec{\gamma}_{\mathbb{I}} + \vec{\gamma}_Z &= -\vec{\gamma}_{\mathbb{R}} - \vec{\gamma}_{\mathbb{I}} - \vec{\gamma}_Z \\
|\vec{\gamma}| &= |\vec{\bar{\gamma}}| \\
\langle \vec{\gamma} \rangle &= \langle \vec{\bar{\gamma}} \rangle \pm \pi \\
[\vec{\gamma}] &= [\vec{\bar{\gamma}}] \pm \pi \\
\vec{\gamma}_{\mathbb{R}} &= -\vec{\bar{\gamma}}_{\mathbb{R}} \\
\vec{\gamma}_{\mathbb{I}} &= -\vec{\bar{\gamma}}_{\mathbb{I}} \\
\vec{\gamma}_Z &= -\vec{\bar{\gamma}}_Z,
\end{aligned} \tag{38}$$

$\forall \vec{\gamma} \in \tilde{S}_{\bar{q}}, \forall \vec{\bar{\gamma}} \in \tilde{S}_{\bar{q}}$, for the 3D-PPS P-symmetry constraint of eq. (85) in [43].

The spontaneously selected superfluid order parameters [42, 43] that comprise $\vec{S}_{\bar{q}}$ and $\vec{\bar{S}}_{\bar{q}}$ transform in such a way that $\vec{S}_{\bar{q}}$ and $\vec{\bar{S}}_{\bar{q}}$ must have a vortical flow motion pattern about $\vec{S}_{\bar{q}}$ and $\vec{\bar{S}}_{\bar{q}}$, respectively—*this is a fundamental and paramount constraint of our developing OTS*. The vorticity of $\vec{S}_{\bar{q}}$ and $\vec{\bar{S}}_{\bar{q}}$ may be rotational or irrotational, depending on the desired application. See Figure 4 for an example depiction of $\tilde{S}_{\bar{q},\bar{q}}$, along with $\vec{S}_{\bar{q},\bar{q}}$ and $\vec{\bar{S}}_{\bar{q},\bar{q}}$. Furthermore, the OTS’s flexibility grants us the option to equip $\tilde{S}_{\bar{q},\bar{q}}$ with its own 3D-OPS layer for an *additional* degree of representation because $\tilde{S}_{\bar{q},\bar{q}} \subset Y_-$ and we can always equip sub-structures of Y with 3D-OPSs.

At this point, we’ve introduced, defined, and assembled a *preliminary* construction of the OTS-Vortex $\tilde{S}_{\bar{q},\bar{q}}$ from the OTS-Vortex Foundation $\vec{S}_{\bar{q},\bar{q}}$ and the OTS-Tube $\vec{\bar{S}}_{\bar{q},\bar{q}}$ for the $q\bar{q}$ dipole in Y that is confined to T^1 , where $\tilde{S}_{\bar{q},\bar{q}}$ comprises the Quark-OTS-Vortex $\vec{S}_{\bar{q}}$ and Antiquark-OTS-Vortex $\vec{\bar{S}}_{\bar{q}}$, which are dual, inverse, opposite, and reverse topological sub-structures that are interdependent for encoding fermion spatial states—all of this is consistent with the quark confinement topology and baryon-antibaryon duality of [42, 43, 44].

3.3 A Fibonacci example application of open topological strings

Now, lets stop for a moment to consider one simple example on how one could conceivably construct and interpret some of $\tilde{S}_{\bar{q},\bar{q}}$ ’s energy and

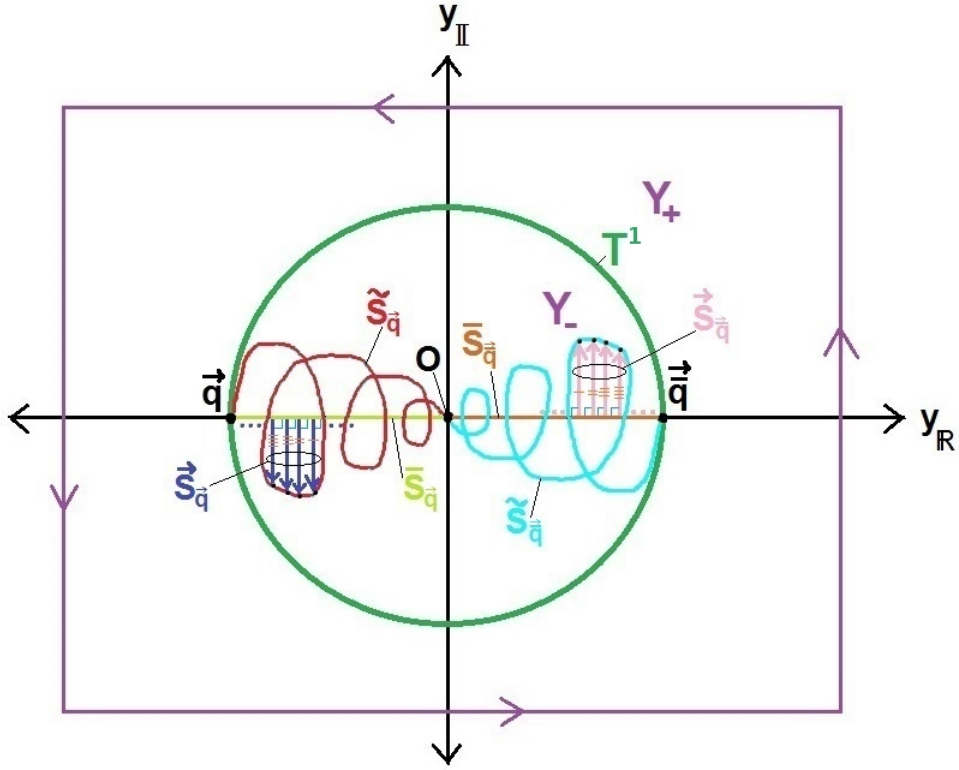


Fig. 4: An example depiction of the OTS-Tube $\vec{S}_{\bar{q},q}$, the OTS-Vortex Foundation $\vec{S}_{q,\bar{q}}$, and the OTS-Vortex $\vec{S}_{\bar{q},q}$ for the spatial states of the $q\bar{q}$ dipole that is confined to T^1 . $T^1 \subset Y$ is simultaneously dual to both $Y_- \subset Y$ and $Y_+ \subset Y$ 3-branes [42, 43, 44].

resonance states in terms of the Fibonacci sequence and spiral.

First, suppose there exists the dual 3D-PPS sets

$$\begin{aligned}\bar{F}_{\bar{q}} \subset \bar{S}_{\bar{q}} &\equiv \{\vec{y}_1, \vec{y}_2, \vec{y}_3, \vec{y}_5, \vec{y}_8, \dots\} \\ \bar{F}_{\bar{q}} \subset \bar{S}_{\bar{q}} &\equiv \{\vec{y}_1, \vec{y}_2, \vec{y}_3, \vec{y}_5, \vec{y}_8, \dots\}\end{aligned}\quad (39)$$

whose location elements satisfy the OTS-Tube 3D-PPS antisymmetric duality constraints of eq. (21), with the additional ‘‘Fibonacci-scaled 3D-PPS amplitude constraints’’

$$\begin{aligned}|\vec{y}_1| &\equiv |\vec{y}_1| \equiv \frac{1}{2}|\vec{y}_2| \equiv \frac{1}{2}|\vec{y}_2| \equiv \frac{1}{3}|\vec{y}_3| \equiv \frac{1}{3}|\vec{y}_3| \\ &\equiv \frac{1}{5}|\vec{y}_5| \equiv \frac{1}{5}|\vec{y}_5| \equiv \frac{1}{8}|\vec{y}_8| \equiv \frac{1}{8}|\vec{y}_8| \equiv \dots,\end{aligned}\quad (40)$$

such that $|\vec{y}_n| \leq d_{q\bar{q}}$, the ‘‘uniform and dual 3D-PPS phase constraints’’

$$\begin{aligned}\langle \vec{y}_1 \rangle &\equiv \langle \vec{y}_1 \rangle \pm \pi \equiv \langle \vec{y}_2 \rangle \equiv \langle \vec{y}_2 \rangle \pm \pi \equiv \langle \vec{y}_3 \rangle \\ &\equiv \langle \vec{y}_3 \rangle \pm \pi \equiv \langle \vec{y}_5 \rangle \equiv \langle \vec{y}_5 \rangle \pm \pi \equiv \langle \vec{y}_8 \rangle \\ &\equiv \langle \vec{y}_8 \rangle \pm \pi \equiv \dots,\end{aligned}\quad (41)$$

and the ‘‘uniform and dual 3D-PPS inclination constraints’’

$$\begin{aligned}[\vec{y}_1] &\equiv [\vec{y}_1] \pm \pi \equiv [\vec{y}_2] \equiv [\vec{y}_2] \pm \pi \equiv [\vec{y}_3] \\ &\equiv [\vec{y}_3] \pm \pi \equiv [\vec{y}_5] \equiv [\vec{y}_5] \pm \pi \equiv [\vec{y}_8] \\ &\equiv [\vec{y}_8] \pm \pi \equiv \dots.\end{aligned}\quad (42)$$

Second, suppose that for the Fibonacci-scaled dual 3D-PPSs of eq. (39) there exist the corresponding dual 3D-OPS sets

$$\begin{aligned}\vec{F}_{\bar{q}} \subset \vec{S}_{\bar{q}} &\equiv \{\vec{\psi}_{\rightarrow}(\vec{y}_1), \vec{\psi}_{\rightarrow}(\vec{y}_2), \vec{\psi}_{\rightarrow}(\vec{y}_3), \vec{\psi}_{\rightarrow}(\vec{y}_5), \vec{\psi}_{\rightarrow}(\vec{y}_8), \dots\} \\ \vec{F}_{\bar{q}} \subset \vec{S}_{\bar{q}} &\equiv \{\vec{\psi}_{\rightarrow}(\vec{y}_1), \vec{\psi}_{\rightarrow}(\vec{y}_2), \vec{\psi}_{\rightarrow}(\vec{y}_3), \vec{\psi}_{\rightarrow}(\vec{y}_5), \vec{\psi}_{\rightarrow}(\vec{y}_8), \dots\}\end{aligned}\quad (43)$$

whose topological deformation elements satisfy the OTS-Vortex Foundation 3D-OPS antisymmetric duality constraints of eq. (32), with the additional ‘‘Fibonacci-scaled 3D-OPS amplitude constraints’’

$$\begin{aligned}|\vec{\psi}_{\rightarrow}(\vec{y}_1)| &\equiv |\vec{\psi}_{\rightarrow}(\vec{y}_1)| \equiv \frac{1}{2}|\vec{\psi}_{\rightarrow}(\vec{y}_2)| \equiv \frac{1}{2}|\vec{\psi}_{\rightarrow}(\vec{y}_2)| \\ &\equiv \frac{1}{3}|\vec{\psi}_{\rightarrow}(\vec{y}_3)| \equiv \frac{1}{3}|\vec{\psi}_{\rightarrow}(\vec{y}_3)| \equiv \frac{1}{5}|\vec{\psi}_{\rightarrow}(\vec{y}_5)| \\ &\equiv \frac{1}{5}|\vec{\psi}_{\rightarrow}(\vec{y}_5)| \equiv \frac{1}{8}|\vec{\psi}_{\rightarrow}(\vec{y}_8)| \equiv \frac{1}{8}|\vec{\psi}_{\rightarrow}(\vec{y}_8)| \\ &\equiv \dots,\end{aligned}\quad (44)$$

the “uniform and dual 3D-OPS phase constraints”

$$\begin{aligned}
\langle \vec{\psi}_{\rightarrow}(\vec{y}_1) \rangle &\equiv \langle \vec{\psi}_{\rightarrow}(\vec{y}_1) \rangle \pm \pi \equiv \langle \vec{\psi}_{\rightarrow}(\vec{y}_2) \rangle &\equiv \langle \vec{\psi}_{\rightarrow}(\vec{y}_2) \rangle \pm \pi \\
&\equiv \langle \vec{\psi}_{\rightarrow}(\vec{y}_3) \rangle &\equiv \langle \vec{\psi}_{\rightarrow}(\vec{y}_3) \rangle \pm \pi \equiv \langle \vec{\psi}_{\rightarrow}(\vec{y}_5) \rangle \\
&\equiv \langle \vec{\psi}_{\rightarrow}(\vec{y}_5) \rangle \pm \pi \equiv \langle \vec{\psi}_{\rightarrow}(\vec{y}_8) \rangle &\equiv \langle \vec{\psi}_{\rightarrow}(\vec{y}_8) \rangle \pm \pi \\
&\equiv \dots ,
\end{aligned} \tag{45}$$

and the “uniform and dual 3D-OPS inclination constraints”

$$\begin{aligned}
[\vec{\psi}_{\rightarrow}(\vec{y}_1)] &\equiv [\vec{\psi}_{\rightarrow}(\vec{y}_1)] \pm \pi \equiv [\vec{\psi}_{\rightarrow}(\vec{y}_2)] &\equiv [\vec{\psi}_{\rightarrow}(\vec{y}_2)] \pm \pi \\
&\equiv [\vec{\psi}_{\rightarrow}(\vec{y}_3)] &\equiv [\vec{\psi}_{\rightarrow}(\vec{y}_3)] \pm \pi \equiv [\vec{\psi}_{\rightarrow}(\vec{y}_5)] \\
&\equiv [\vec{\psi}_{\rightarrow}(\vec{y}_5)] \pm \pi \equiv [\vec{\psi}_{\rightarrow}(\vec{y}_8)] &\equiv [\vec{\psi}_{\rightarrow}(\vec{y}_8)] \pm \pi \\
&\equiv \dots .
\end{aligned} \tag{46}$$

Thus, given the Fibonacci-based OTS-Tube and OTS-Vortex Foundation constructions of eqs. (39–46), there exists the dual 3D-PPS sets

$$\begin{aligned}
\tilde{F}_{\vec{q}} \subset \tilde{S}_{\vec{q}} &\equiv \{\vec{\gamma}_1, \vec{\gamma}_2, \vec{\gamma}_3, \vec{\gamma}_5, \vec{\gamma}_8, \dots\} \\
\tilde{F}_{\vec{q}} \subset \tilde{S}_{\vec{q}} &\equiv \{\vec{\gamma}_1, \vec{\gamma}_2, \vec{\gamma}_3, \vec{\gamma}_5, \vec{\gamma}_8, \dots\}
\end{aligned} \tag{47}$$

whose location elements satisfy the OTS-Vortex 3D-PPS antisymmetric duality constraints of eq. (21), with the additional “Fibonacci-scaled 3D-PPS amplitude constraints”

$$\begin{aligned}
|\vec{\gamma}_1| &\equiv |\vec{\gamma}_1| \equiv \frac{1}{2}|\vec{\gamma}_2| \equiv \frac{1}{2}|\vec{\gamma}_2| \equiv \frac{1}{3}|\vec{\gamma}_3| \equiv \frac{1}{3}|\vec{\gamma}_3| \\
&\equiv \frac{1}{5}|\vec{\gamma}_5| \equiv \frac{1}{5}|\vec{\gamma}_5| \equiv \frac{1}{8}|\vec{\gamma}_8| \equiv \frac{1}{8}|\vec{\gamma}_8| \equiv \dots ,
\end{aligned} \tag{48}$$

the “uniform and dual 3D-PPS phase constraints”

$$\begin{aligned}
\langle \vec{\gamma}_1 \rangle &\equiv \langle \vec{\gamma}_1 \rangle \pm \pi \equiv \langle \vec{\gamma}_2 \rangle &\equiv \langle \vec{\gamma}_2 \rangle \pm \pi \equiv \langle \vec{\gamma}_3 \rangle \\
&\equiv \langle \vec{\gamma}_3 \rangle \pm \pi \equiv \langle \vec{\gamma}_5 \rangle &\equiv \langle \vec{\gamma}_5 \rangle \pm \pi \equiv \langle \vec{\gamma}_8 \rangle \\
&\equiv \langle \vec{\gamma}_8 \rangle \pm \pi \equiv \dots ,
\end{aligned} \tag{49}$$

and the “uniform and dual 3D-PPS inclination constraints”

$$\begin{aligned}
[\vec{\gamma}_1] &\equiv [\vec{\gamma}_1] \pm \pi \equiv [\vec{\gamma}_2] &\equiv [\vec{\gamma}_2] \pm \pi \equiv [\vec{\gamma}_3] \\
&\equiv [\vec{\gamma}_3] \pm \pi \equiv [\vec{\gamma}_5] &\equiv [\vec{\gamma}_5] \pm \pi \equiv [\vec{\gamma}_8] \\
&\equiv [\vec{\gamma}_8] \pm \pi \equiv \dots .
\end{aligned} \tag{50}$$

The next step is to define $\tilde{S}_{\vec{q},\vec{q}}$'s flow vorticity in Y_- at the Fibonacci-scaled 3D-PPSs of eq. (47). Thus, the superfluidic motion velocity field is defined using the triplex numbers of [43] for the $\tilde{S}_{\vec{q},\vec{q}}$'s Fibonacci-scaled 3D-PPSs of eq. (47) as

$$\begin{aligned} v(\vec{\gamma}_i) &\equiv v(\vec{\gamma}_i)_{\mathbb{R}} + v(\vec{\gamma}_i)_{\mathbb{I}} + v(\vec{\gamma}_i)_Z \equiv (v(\vec{\gamma}_i)_{\mathbb{R}}, v(\vec{\gamma}_i)_{\mathbb{I}}, v(\vec{\gamma}_i)_Z)_C \\ &\equiv (|v(\vec{\gamma}_i)|, \langle v(\vec{\gamma}_i) \rangle, [v(\vec{\gamma}_i)])_S \end{aligned} \quad (51)$$

with the duality constraints

$$\begin{aligned} v(\vec{\gamma}_i)_{\mathbb{R}} + v(\vec{\gamma}_i)_{\mathbb{I}} + v(\vec{\gamma}_i)_Z &\equiv -v(\vec{\gamma}_i)_{\mathbb{R}} - v(\vec{\gamma}_i)_{\mathbb{I}} - v(\vec{\gamma}_i)_Z \\ |v(\vec{\gamma}_i)| &\equiv |v(\vec{\gamma}_i)| \\ \langle v(\vec{\gamma}_i) \rangle &\equiv \langle v(\vec{\gamma}_i) \rangle \pm \pi \\ [v(\vec{\gamma}_i)] &\equiv [v(\vec{\gamma}_i)] \pm \pi \\ v(\vec{\gamma}_i)_{\mathbb{R}} &\equiv -v(\vec{\gamma}_i)_{\mathbb{R}} \\ v(\vec{\gamma}_i)_{\mathbb{I}} &\equiv -v(\vec{\gamma}_i)_{\mathbb{I}} \\ v(\vec{\gamma}_i)_Z &\equiv -v(\vec{\gamma}_i)_Z, \end{aligned} \quad (52)$$

$\forall \vec{\gamma}_i \in \tilde{F}_{\vec{q}}$ (and clearly $\forall \vec{\gamma}_i \in \tilde{F}_{\vec{q}}$). Therefore, $\tilde{S}_{\vec{q}}$'s flow vorticity at the Fibonacci-scaled 3D-PPSs of eq. (47) is defined as

$$\begin{aligned} \vec{\omega}(\vec{\gamma}_i) &\equiv \left(\frac{\partial}{\partial \vec{\gamma}_{i\mathbb{R}}}, \frac{\partial}{\partial \vec{\gamma}_{i\mathbb{I}}}, \frac{\partial}{\partial \vec{\gamma}_{iZ}} \right) \times (v(\vec{\gamma}_i)_{\mathbb{R}}, v(\vec{\gamma}_i)_{\mathbb{I}}, v(\vec{\gamma}_i)_Z) \\ &\equiv \left(\frac{\partial v(\vec{\gamma}_i)_Z}{\partial \vec{\gamma}_{i\mathbb{I}}} - \frac{\partial v(\vec{\gamma}_i)_{\mathbb{I}}}{\partial \vec{\gamma}_{iZ}}, \frac{\partial v(\vec{\gamma}_i)_{\mathbb{R}}}{\partial \vec{\gamma}_{iZ}} - \frac{\partial v(\vec{\gamma}_i)_Z}{\partial \vec{\gamma}_{i\mathbb{R}}}, \frac{\partial v(\vec{\gamma}_i)_{\mathbb{I}}}{\partial \vec{\gamma}_{i\mathbb{R}}} - \frac{\partial v(\vec{\gamma}_i)_{\mathbb{R}}}{\partial \vec{\gamma}_{i\mathbb{I}}} \right), \end{aligned} \quad (53)$$

which is the *curl* of the velocity fields of eq. (51) and dual to $\tilde{S}_{\vec{q}}$ in accordance to eq. (52). See Figure 5 for the depiction of this Fibonacci example application of $\tilde{S}_{\vec{q},\vec{q}}$ in Y_- . Certainly, it is possible to express eq. (53) in the triplex form of [43] with triplex multiplication.

Moreover, we again stress that this is only one Fibonacci sequence encoding method among many possible methods. Therefore, it may be beneficial to explore such alternatives in future research.

4 Closed topological strings for boson temporal states

Here, we introduce, define, and assemble a CTS and its temporal state space for the boson features of the $q\bar{q}$ dipole that is confined to the IHR T^1 [42] using the triplex encoding framework of [43]. In general, the CTS contains two distinct information sub-structures: the

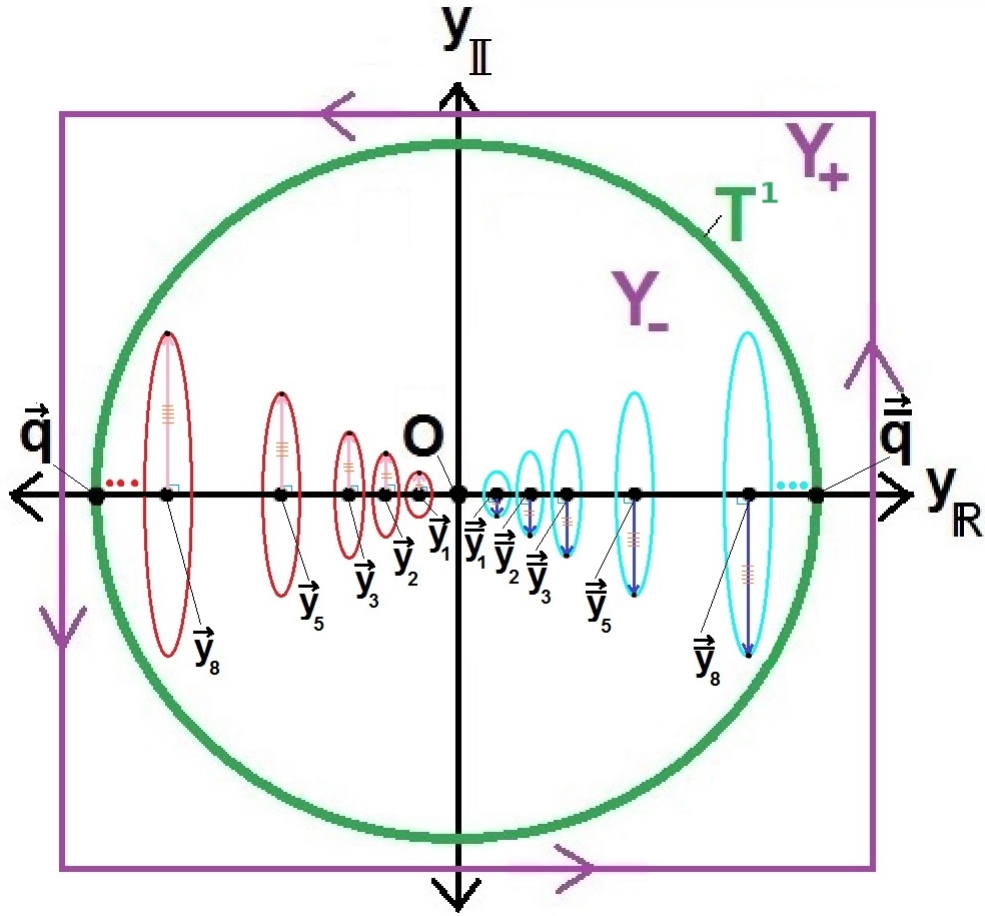


Fig. 5: One initial example on how to apply the Fibonacci sequence to interpret the spatial energy and resonance states of $\tilde{S}_{\vec{q},\vec{q}}$ for the $q\bar{q}$ dipole that is confined to T^1 , where the Fibonacci-scaled 3D-PPSs of $\tilde{S}_{\vec{q},\vec{q}}$ contain velocity field curl and flow vorticity for superfluidic motion. This is a new and general idea that may have lots of encoding applications to non-linear structures in nature, such as superconductors, spiral galaxies, and more.

1. *Closed Topological String Ring* (CTS-Ring), a *non-linear* information sub-structure; and
2. *Closed Topological String Helix* (CTS-Helix), a *non-linear* information sub-structure.

Here, we identify, construct, and discuss both CTS sub-structures and their interdependence.

4.1 Closed topological string rings

Here, the 1-sphere IHR T^1 is relabeled as a CTS-Ring for notational consistency: it's definition is rewritten as

$$\mathring{T}_{\vec{q}, \vec{q}} \equiv \mathring{T}(\vec{q}, \vec{q}) \equiv T^1 \equiv \{\vec{y} \in Y : |\vec{y}| = \epsilon = |\vec{q}| = |\vec{q}|\}. \quad (54)$$

Now, due to the fact that $\mathring{T}_{\vec{q}, \vec{q}}$ is continuous because it is a smooth 1-sphere curve and a 3D-PPS sub-space of Y , then the *CTS-Ring 3D-PPS cardinality* is expressed as

$$|\mathring{T}_{\vec{q}, \vec{q}}| \equiv |\mathring{T}(\vec{q}, \vec{q})| \equiv \infty \quad (55)$$

for an *infinite* number of 3D-PPSs within $\mathring{T}_{\vec{q}, \vec{q}}$, even though the *CTS-Ring 3D-PPS length* is expressed as

$$||\mathring{T}_{\vec{q}, \vec{q}}|| \equiv ||\mathring{T}(\vec{q}, \vec{q})|| \equiv 2\pi d_{q\bar{q}} \equiv 2\pi\epsilon \quad (56)$$

for the *finite* circumference.

There is no need to try to figure out how to split $\mathring{T}_{\vec{q}, \vec{q}}$ into the dual left-handed and right-handed components like we did with $\mathring{S}_{\vec{q}, \vec{q}}$ because the relevant time-reversal and parity-symmetry transformations of eqs. (85–86) in [43] have already been applied to demonstrate the existence of counterbalancing 3D-PPSs along $\mathring{T}_{\vec{q}, \vec{q}}$ with opposite, inverse, and reverse features. For example, in eq. (5) we recall that the 3D-PPSs $\vec{q}, \vec{q} \in \mathring{T}_{\vec{q}, \vec{q}}$ are “directionally separated” along $\mathring{T}_{\vec{q}, \vec{q}}$ by π in terms of both phase and inclination [43]; this utilization of π is paramount to the work of [42, 43] and exemplifies a key property of nature. Therefore, if the 3D-PPSs $\vec{q}, \vec{q} \in \mathring{T}_{\text{vecq}, \vec{q}}$ are “directionally separated” along $\mathring{T}_{\vec{q}, \vec{q}}$ by π in this fashion, then certainly

the OTS-Tube 3D-PPS antisymmetric duality constraints of eq. (21) apply to this context as *CTS-Ring 3D-PPS antisymmetric duality constraints*, $\forall \vec{y}, \vec{y} \in \overset{\circ}{T}_{\vec{q}, \vec{q}}$.

Hence, at this point, we've introduced, defined, and assembled the CTS-Ring $\overset{\circ}{T}_{\vec{q}, \vec{q}}$ for the $q\bar{q}$ dipole in Y that is indeed confined to $\overset{\circ}{T}_{\vec{q}, \vec{q}} \equiv T^1$, where counter-balancing 3D-PPSs along $\overset{\circ}{T}_{\vec{q}, \vec{q}}$ contain dual, inverse, opposite, and reverse locations that are interdependent—all of this is consistent with the quark confinement topology and baryon-antibaryon duality of [42, 43].

4.2 Closed topological string helices

Here, we assemble the CTS-Helix for the $q\bar{q}$ dipole by equipping the CTS-Ring $\overset{\circ}{T}_{\vec{q}, \vec{q}}$ with a 3D-OPS layer of fractional statistics for the “generic” topological deformations of [43], which upgrades the framework of [42]. In fact, as we will show, the CTS-Helix is also consistent with the CPT-Theorem implementation of [42, 43], where the topological deformations that form the foundation of the CTS-Helix exhibit opposite, inverse, and reverse features that are also directionally separated along $\overset{\circ}{T}_{\vec{q}, \vec{q}}$ by π .

Now, from eq. (50) in [43] we know that Y can be assigned a 3D-OPS layer for topological deformations. Thus, because $\overset{\circ}{T}_{\vec{q}, \vec{q}} \subset Y$, we know that eq. (50) in [43] applies to $\overset{\circ}{T}_{\vec{q}, \vec{q}}$. Hence, the first step is to define the *topological 1-sphere of 3D-OPSs* for $\overset{\circ}{T}_{\vec{q}, \vec{q}}$ as

$$\vec{T}_{\vec{q}, \vec{q}} \equiv \vec{T}(\vec{q}, \vec{q}) \equiv \bigcup_{\vec{y} \in \overset{\circ}{T}_{\vec{q}, \vec{q}}} \vec{\psi}_{\rightarrow}(\vec{y}), \quad (57)$$

which assigns $\overset{\circ}{T}_{\vec{q}, \vec{q}}$'s 3D-OPS layer for topological deformations, where $\vec{\psi}_{\rightarrow}(\vec{y})$ is the 3D-OPS in the 3D-OPSS $\vec{\Phi}_{\rightarrow}(\vec{y})$ at $\vec{y} \in \overset{\circ}{T}_{\vec{q}, \vec{q}}$, such that $\vec{\psi}_{\rightarrow}(\vec{y}) \in \vec{\Phi}_{\rightarrow}(\vec{y})$; $\vec{T}_{\vec{q}, \vec{q}}$ of eq. (57) is called the *CTS-Helix Foundation*, which is a continuous ordered 3D-OPS set, such that $\vec{T}_{\vec{q}, \vec{q}}$'s infinite cardinality is

$$|\vec{T}_{\vec{q}, \vec{q}}| \equiv |\overset{\circ}{T}_{\vec{q}, \vec{q}}| \equiv \infty, \quad (58)$$

and $\vec{T}_{\vec{q}, \vec{q}}$'s finite circumference length is

$$||\vec{T}_{\vec{q}, \vec{q}}|| \equiv ||\overset{\circ}{T}_{\vec{q}, \vec{q}}|| \equiv 2\pi d_{q\bar{q}} \equiv 2\pi\epsilon. \quad (59)$$

Figure 6 depicts a 3D-OPS layer assignment to the CTS-Ring $\mathring{T}_{\vec{q},\vec{q}}$ for topological deformations—this method is used to build the CTS-Helix Foundation $\vec{T}_{\vec{q},\vec{q}}$ for the CTS-Helix $\tilde{T}_{\vec{q},\vec{q}}$ definition in the upcoming eq. (60).

Therefore, the 3D-PPSs of $\mathring{T}_{\vec{q},\vec{q}}$ and the corresponding 3D-OPSs of $\vec{T}_{\vec{q},\vec{q}}$ are sequentially summed to define the CTS-Helix $\tilde{T}_{\vec{q},\vec{q}}$ for the $q\bar{q}$ dipole, which is a *topological 3D helix space of 3D-OPSs*, as

$$\tilde{T}_{\vec{q},\vec{q}} \subset Y \equiv \tilde{T}(\vec{q}, \vec{q}) \subset Y \equiv \bigcup_{\vec{y} \in \mathring{T}_{\vec{q},\vec{q}}} \vec{y} + \vec{\psi}_{\rightarrow}(\vec{y}) \equiv \bigcup_{\vec{y} \in \vec{T}_{\vec{q},\vec{q}}} \gamma(\vec{y}), \quad (60)$$

where

$$\vec{\gamma} \equiv \gamma(\vec{y}) \equiv \vec{y} + \vec{\psi}_{\rightarrow}(\vec{y}), \quad \forall \vec{y} \in \mathring{T}_{\vec{q},\vec{q}}, \quad \forall \vec{\psi}_{\rightarrow}(\vec{y}) \in \vec{T}_{\vec{q},\vec{q}}, \quad (61)$$

such that $\vec{\gamma} \in \tilde{T}_{\vec{q},\vec{q}} \subset Y$. At this point, we do not know the exact structure, shape, or length of $\tilde{T}_{\vec{q},\vec{q}}$ because it depends on a number of features (that we will soon discuss), but we do know that it must somehow wind around $\mathring{T}_{\vec{q},\vec{q}}$, has some finite length $|\tilde{T}_{\vec{q},\vec{q}}|$, such that $|\tilde{T}_{\vec{q},\vec{q}}| > 2\pi d_{q\bar{q}}$, and bares an infinite cardinality $|\tilde{T}_{\vec{q},\vec{q}}| \equiv \infty$ —for now, these preliminary and approximate constraints are all that we need to be aware of.

Now similarly to the $\mathring{T}_{\vec{q},\vec{q}}$ case of Section 4.1, there is no need to try to split $\vec{T}_{\vec{q},\vec{q}}$ or $\tilde{T}_{\vec{q},\vec{q}}$ into the dual left-handed and right-handed components because the relevant time-reversal and parity-symmetry transformations of eqs. (85–86) in [43] apply to demonstrate the existence of counterbalancing 3D-OPSs along $\vec{T}_{\vec{q},\vec{q}}$, which result in the counterbalancing 3D-PPSs along $\tilde{T}_{\vec{q},\vec{q}}$ —both $\vec{T}_{\vec{q},\vec{q}}$ and $\tilde{T}_{\vec{q},\vec{q}}$ have opposite, inverse, and reverse features. For this, the OTS-Vortex Foundation 3D-OPS antisymmetric duality constraints of eq. (32) apply to $\vec{T}_{\vec{q},\vec{q}}$ as *CTS-Helix Foundation 3D-OPS antisymmetric duality constraints* $\forall \vec{\psi}_{\rightarrow}(\vec{y}), \vec{p}s_{i\rightarrow}(\vec{y}) \in \vec{T}_{\vec{q},\vec{q}}$ because their phases and inclinations are directionally separated by π . Similarly, the OTS-Vortex 3D-PPS antisymmetric duality constraints of eq. (38) apply to $\tilde{T}_{\vec{q},\vec{q}}$ as *CTS-Helix 3D-PPS antisymmetric duality constraints* $\forall \vec{\gamma}, \vec{\gamma} \in \tilde{T}_{\vec{q},\vec{q}}$.

The spontaneously selected superfluid order parameters that comprise $\vec{T}_{\vec{q},\vec{q}}$ transform in such a way that $\tilde{T}_{\vec{q},\vec{q}}$ must have a helicoidal flow motion pattern about $\mathring{T}_{\vec{q},\vec{q}}$, respectively—*this is a fundamental and paramount*

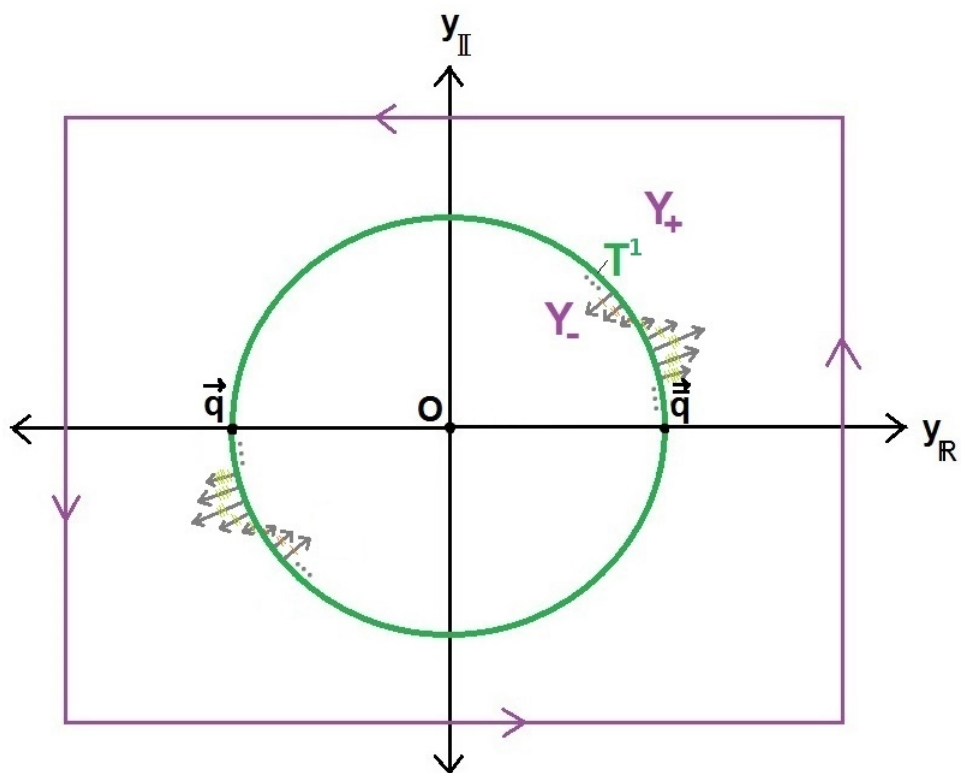


Fig. 6: A 3D-OPS layer is assigned to the 1-sphere IHR T^1 (which has been relabeled as the CTS-Ring $\mathring{T}_{\vec{q}, \vec{q}}$ for notation consistency, so $T^1 \equiv \mathring{T}_{\vec{q}, \vec{q}}$) for topological deformations. This method is used to build the CTS-Helix Foundation $\vec{T}_{\vec{q}, \vec{q}}$ for the CTS-Helix $\tilde{T}_{\vec{q}, \vec{q}}$.

constraint of our developing CTS. Additionally, this framework’s flexibility grants us the option to further equip $\tilde{T}_{\bar{q},\bar{q}}$ with its own 3D-OPS layer for an *additional* degree of representation. In order to mathematically implement and experimentally apply this concept of helicoidal flow, this emerging model of $\tilde{T}_{\bar{q},\bar{q}}$ requires further scientific collaboration, scrutiny, and investigation—an excellent facet of exploration for future research. See Figure 7 for an example depiction of $\tilde{T}_{\bar{q},\bar{q}}$, along with $\vec{T}_{\bar{q},\bar{q}}$ and $\overset{\circ}{T}_{\bar{q},\bar{q}}$.

At this point, we’ve introduced, defined, and assembled a *preliminary* construction of the CTS-Ring $\overset{\circ}{T}_{\bar{q},\bar{q}}$, the CTS-Helix Foundation $\vec{T}_{\bar{q},\bar{q}}$, and the CTS-Helix $\tilde{T}_{\bar{q},\bar{q}}$ for the $q\bar{q}$ dipole in Y , where the counterbalancing features are dual, inverse, opposite, and reverse topological sub-structures that are interdependent for boson temporal states—all of this is consistent with the quark confinement topology and baryon-antibaryon duality of [42, 43]. See Table 1 for a summary of the preliminary topological string theory structures introduced in this paper.

Table 1: A summary of the topological string structures for the $q\bar{q}$ dipole, which include the OTS and CTS.

Name	Symbol	Composition
OTS-Tube	$\vec{S}_{\bar{q},\bar{q}}$	3D-PPS
OTS-Vortex Foundation	$\tilde{S}_{\bar{q},\bar{q}}$	3D-OPS
OTS-Vortex	$\overset{\circ}{S}_{\bar{q},\bar{q}}$	3D-PPS
CTS-Ring	$\vec{T}_{\bar{q},\bar{q}}$	3D-PPS
CTS-Helix Foundation	$\tilde{T}_{\bar{q},\bar{q}}$	3D-OPS
CTS-Helix	$\overset{\circ}{T}_{\bar{q},\bar{q}}$	3D-PPS

5 Initiating the iso-topic liftings

Finally, it is time to deploy Santilli’s iso-numbers [36, 37, 38, 39, 40, 45] to iso-topically lift the OTS of Section 3 and the CTS of Section 4. For this *preliminary* implementation, we follow Santilli’s iso-methodology [36, 37, 38, 39, 40, 45] and execute the following procedure:

1. First, we select some positive-definite iso-unit $\hat{r} > 0$ with the corresponding inverse $\hat{\kappa} = \frac{1}{\hat{r}} > 0$, which will be used to iso-topically lift the triplex space Y (and all of its sub-spaces) to the iso-triplex space $Y^{\hat{r}}$

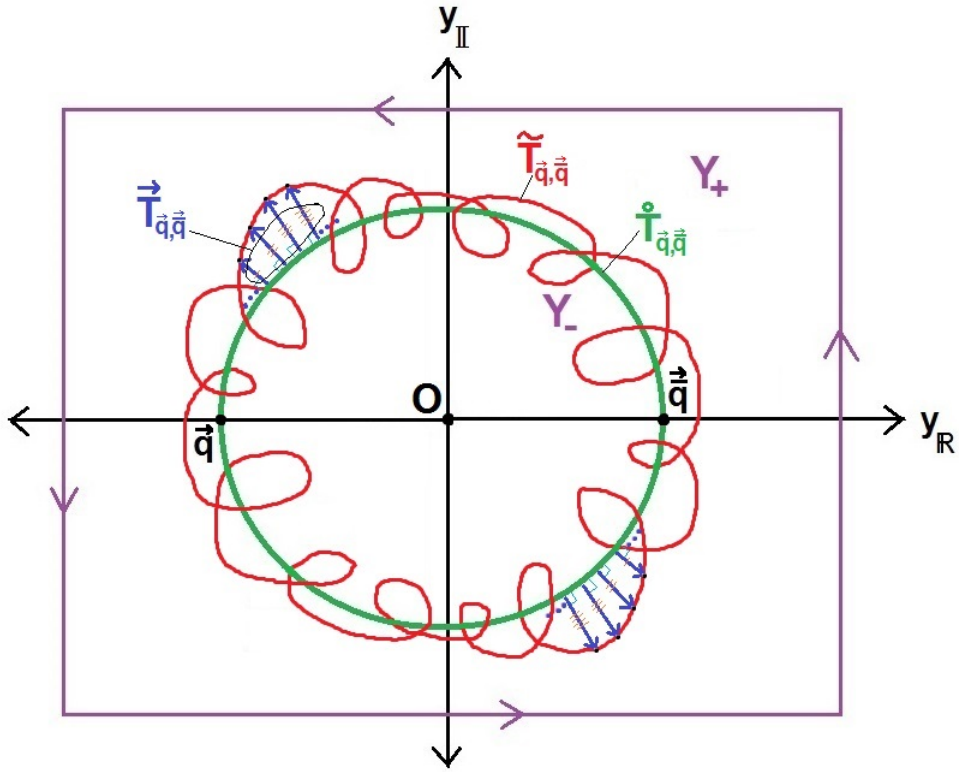


Fig. 7: An example depiction of the CTS-Ring $\hat{T}_{\vec{q}, \vec{q}} \equiv T^1$, the CTS-Helix Foundation $\hat{T}_{\vec{q}, \vec{q}}$, and the CTS-Helix $\tilde{T}_{\vec{q}, \vec{q}}$ for the temporal states of the $q\bar{q}$ dipole that is confined to $\hat{T}_{\vec{q}, \vec{q}}$. $\hat{T}_{\vec{q}, \vec{q}} \subset Y$ is simultaneously dual to both $Y_- \subset Y$ and $Y_+ \subset Y$ [42, 43].

via the transition $Y \rightarrow Y^{\hat{r}}$, such that the $q\bar{q}$ dipole that is confined to $T^1 \subset Y$ is iso-topically lifted to the $\hat{q}\hat{\bar{q}}$ iso-dipole that is confined to $\hat{T}^1|^{\hat{r}} \subset Y^{\hat{r}}$. We note that in this application, we use \hat{r} to lift both the 3D-PPSs and the 3D-OPSs, but we could optionally select different iso-units for both cases.

2. Second, we use \hat{r} to iso-topically lift the OTS-Tube $\bar{S}_{\bar{q},\bar{q}}$ of eq. (9) via the transition

$$\delta(\bar{S}_{\bar{q},\bar{q}}, \hat{r}) : \bar{S}_{\bar{q},\bar{q}} \rightarrow \bar{S}_{\bar{q},\bar{q}}^{\hat{r}} \quad (62)$$

to define the *Iso-OTS-Tube* $\bar{S}_{\bar{q},\bar{q}}^{\hat{r}}$, which similarly applies to the sub-structures and inherent characteristics of eqs. (10–21); $\bar{S}_{\bar{q},\bar{q}}$ and $\bar{S}_{\bar{q},\bar{q}}^{\hat{r}}$ are locally iso-morphic.

3. Third, we use \hat{r} to iso-topically lift the OTS-Vortex Foundation $\vec{S}_{\bar{q},\bar{q}}$ of eq. (22) via the transition

$$\delta(\vec{S}_{\bar{q},\bar{q}}, \hat{r}) : \vec{S}_{\bar{q},\bar{q}} \rightarrow \vec{S}_{\bar{q},\bar{q}}^{\hat{r}} \quad (63)$$

to define the *Iso-OTS-Vortex Foundation* $\vec{S}_{\bar{q},\bar{q}}^{\hat{r}}$, which similarly applies to the sub-structures and inherent characteristics of eqs. (23–24) and eqs. (27–32); $\vec{S}_{\bar{q},\bar{q}}$ and $\vec{S}_{\bar{q},\bar{q}}^{\hat{r}}$ are locally iso-morphic.

4. Fourth, we use \hat{r} to iso-topically lift the OTS-Vortex $\tilde{S}_{\bar{q},\bar{q}}$ of eq. (25) via the transition

$$\delta(\tilde{S}_{\bar{q},\bar{q}}, \hat{r}) : \tilde{S}_{\bar{q},\bar{q}} \rightarrow \tilde{S}_{\bar{q},\bar{q}}^{\hat{r}} \quad (64)$$

to define the *Iso-OTS-Vortex* $\tilde{S}_{\bar{q},\bar{q}}^{\hat{r}}$, which similarly applies to the sub-structures and inherent characteristics of eqs. (33–38); $\tilde{S}_{\bar{q},\bar{q}}$ and $\tilde{S}_{\bar{q},\bar{q}}^{\hat{r}}$ are locally iso-morphic.

5. Fifth, we use \hat{r} to iso-topically lift the CTS-Ring $\overset{\circ}{T}_{\bar{q},\bar{q}}$ of eq. (54) via the transition

$$\delta(\overset{\circ}{T}_{\bar{q},\bar{q}}, \hat{r}) : \overset{\circ}{T}_{\bar{q},\bar{q}} \rightarrow \overset{\circ}{T}_{\bar{q},\bar{q}}^{\hat{r}} \quad (65)$$

to define the *Iso-CTS-Ring* $\overset{\circ}{T}_{\bar{q},\bar{q}}^{\hat{r}}$, which similarly applies to the inherent characteristics of eqs. (55–56); $\overset{\circ}{T}_{\bar{q},\bar{q}}$ and $\overset{\circ}{T}_{\bar{q},\bar{q}}^{\hat{r}}$ are locally iso-morphic.

6. Sixth, we use \hat{r} to iso-topically lift the CTS-Helix Foundation $\vec{T}_{\vec{q},\vec{q}}$ of eq. (57) via the transition

$$\delta(\vec{T}_{\vec{q},\vec{q}}, \hat{r}) : \vec{T}_{\vec{q},\vec{q}} \rightarrow \vec{T}_{\vec{q},\vec{q}}^{\hat{r}} \quad (66)$$

to define the *Iso-CTS-Helix Foundation* $\vec{T}_{\vec{q},\vec{q}}^{\hat{r}}$, which similarly applies to the inherent characteristics of eqs. (58–59); $\vec{T}_{\vec{q},\vec{q}}$ and $\vec{T}_{\vec{q},\vec{q}}^{\hat{r}}$ are locally iso-morphic.

7. Seventh, we use \hat{r} to iso-topically lift the CTS-Helix $\tilde{T}_{\vec{q},\vec{q}}$ of eq. (60) via the transition

$$\delta(\tilde{T}_{\vec{q},\vec{q}}, \hat{r}) : \tilde{T}_{\vec{q},\vec{q}} \rightarrow \tilde{T}_{\vec{q},\vec{q}}^{\hat{r}} \quad (67)$$

to define the *Iso-CTS-Helix* $\tilde{T}_{\vec{q},\vec{q}}^{\hat{r}}$, which similarly applies to the inherent characteristics of eq. (61); $\tilde{T}_{\vec{q},\vec{q}}$ and $\tilde{T}_{\vec{q},\vec{q}}^{\hat{r}}$ are locally iso-morphic.

At this point, we can update Table 1 to establish Table 2, which reflects the preliminary TIST structures introduced in this paper.

Table 2: A summary of the TIST structures for the $\hat{q}\hat{q}$ iso-dipole, which include the Iso-OTS and Iso-CTS.

Name	Symbol	Composition
Iso-OTS-Tube	$\vec{S}_{\vec{q},\vec{q}}^{\hat{r}}$	Iso-3D-PPS
Iso-OTS-Vortex Foundation	$\vec{S}_{\vec{q},\vec{q}}^{\hat{r}}$	Iso-3D-OPS
Iso-OTS-Vortex	$\vec{S}_{\vec{q},\vec{q}}^{\hat{r}}$	Iso-3D-PPS
Iso-CTS-Ring	$\vec{T}_{\vec{q},\vec{q}}^{\hat{r}}$	Iso-3D-PPS
Iso-CTS-Helix Foundation	$\vec{T}_{\vec{q},\vec{q}}^{\hat{r}}$	Iso-3D-OPS
Iso-CTS-Helix	$\vec{T}_{\vec{q},\vec{q}}^{\hat{r}}$	Iso-3D-PPS

6 Conclusion

In this preliminary investigation, we started by discussing some limiting aspects of the conventional string theory which operates in the 11D space-time framework [1, 2, 3, 4]. We listed numerous examples of structures in nature that exhibit helical, spiral, and vortical patterns, and proposed that

a string-based unification candidate must be able to encode such patterns by default. From this, we proposed a hypothesis, which conjectured that Santilli's iso-numbers [36, 37, 38, 39, 40, 45] and the IHR [42, 43, 44, 45] may enable us to construct a TIST in the iso-dual 4D space-time IHR topology, which may serve as a topological upgrade to conventional string theory [1, 2, 3, 4]. Consequently, we forged ahead and began to test this hypothesis by engaging triplex numbers and topological deformation order parameters to construct the OTS and CTS for a quark-antiquark dipole in the dual 4D space-time IHR topology [42, 43, 44, 45]. In doing so, we identified one simple example on how the OTS energy and resonance states can be quantified in terms of the well-known Fibonacci sequence for understanding superfluidic motion velocity fields and flow vorticities. Subsequently, we deployed the iso-triplex numbers to iso-topically lift the OTS and CTS to the Iso-OTS and Iso-CTS, respectively, in the iso-dual 4D space-time IHR topology [45].

The initial results of this venture are significant because they seem to support our hypothesis, which aims to reveal the landscape of an alternative unification candidate with low-dimensional iso-mathematics. More precisely, the topological iso-strings are cutting-edge structures that begin to advance Santilli's iso-numbers [36, 37, 38, 39, 40, 45] to new string-based realms of application and exploration. Ultimately, we must develop this TIST to such a degree so that its predictive and representational capabilities may be tested with real-time astronomical data and high-energy physics experiments. Hence, there is much work to be done because this emerging TIST framework is still rudimentary and therefore requires further scrutiny, collaboration, refinement, and generalization via the Scientific Method.

References

- [1] T. Mohaupt. Introduction to string theory. *Quantum Gravity*, page 203, 2003.
- [2] T. Weigand. Introduction to string theory, 2010.
- [3] B. Greene. *The elegant universe: Superstrings, hidden dimensions, and the quest for the ultimate theory*. Vintage, 2000.
- [4] E. Witten. Black holes and quark confinement. *Current Science-Bangalore*, 81(12):1576, 2001.

- [5] N. Cartwright and R. Frigg. String theory under scrutiny. *Physics World*, 20(9):14, 2007.
- [6] L. Smolin and J. Harnad. The trouble with physics: the rise of string theory, the fall of a science, and what comes next. *The Mathematical Intelligencer*, 30(3):66–69, 2008.
- [7] P. Woit. *Not even wrong: the failure of string theory and the search for unity in physical law*. Basic Books, 2006.
- [8] R. Hedrich. The internal and external problems of string theory: A philosophical view. *Journal for General Philosophy of Science*, 38(2):261, 2007.
- [9] K. C. Chou. Low-frequency vibrations of helical structures in protein molecules. *Biochemical Journal*, 209(3):573, 1983.
- [10] K. C. Chou. Low-frequency vibrations of DNA molecules. *Biochemical Journal*, 221(1):27, 1984.
- [11] K. C. Chou. Biological functions of low-frequency vibrations (phonons). 3. helical structures and microenvironment. *Biophysical Journal*, 45(5):881, 1984.
- [12] K. C. Chou. The biological functions of low-frequency vibrations (phonons): 4. resonance effects and allosteric transition. *Biophysical Chemistry*, 20(1):61, 1984.
- [13] K. C. Chou. Low-frequency collective motion in biomacromolecules and its biological functions. *Biophysical Chemistry*, 30(1):3, 1988.
- [14] D. M. Engelman, T. A. Steitz, and A. Goldman. Identifying nonpolar transbilayer helices in amino acid sequences of membrane proteins. *Annual review of biophysics and biophysical chemistry*, 15(1):321–353, 1986.
- [15] S. Padmanabhan, S. Marqusee, T. Ridgeway, T. M. Laue, and R. L. Baldwin. Relative helix-forming tendencies of nonpolar amino acids. 1990.
- [16] K. Iida and G. Baym. Superfluid phases of quark matter. iii. supercurrents and vortices. *Physical Review D*, 66(1):014015, 2002.
- [17] A. A. Abrikosov. Nobel lecture: Type-ii superconductors and the vortex lattice. *Reviews of Modern Physics*, 76(3):975, 2004.
- [18] M. R. Matthews, B. P. Anderson, P. C. Haljan, D. S. Hall, C. E. Wieman, and E. A. Cornell. Vortices in a Bose-Einstein condensate.

- arXiv preprint cond-mat/9908209*, 1999.
- [19] B. P. Anderson, P. C. Haljan, C. A. Regal, D. L. Feder, L. A. Collins, C. W. Clark, and E. A. Cornell. Watching dark solitons decay into vortex rings in a Bose-Einstein condensate. *Physical Review Letters*, 86(14):2926, 2001.
 - [20] J. R. Abo-Shaeer, C. Raman, J. M. Vogels, and W. Ketterle. Observation of vortex lattices in Bose-Einstein condensates. *Science*, 292(5516):476–479, 2001.
 - [21] N. B. Ward. The exploration of certain features of tornado dynamics using a laboratory model. *Journal of the Atmospheric Sciences*, 29(6):1194–1204, 1972.
 - [22] B. H. Fiedler and R. Rotunno. A theory for the maximum wind-speeds in tornado-like vortices. *Journal of the atmospheric sciences*, 43(21):2328–2340, 1986.
 - [23] J. Wurman. The multiple-vortex structure of a tornado. *Weather and forecasting*, 17(3):473–505, 2002.
 - [24] M. Fiorino and R. L. Elsberry. Some aspects of vortex structure related to tropical cyclone motion. *Journal of the atmospheric sciences*, 46(7):975–990, 1989.
 - [25] Y. Wang. Vortex Rossby waves in a numerically simulated tropical cyclone. part i: Overall structure, potential vorticity, and kinetic energy budgets*. *Journal of the atmospheric sciences*, 59(7):1213–1238, 2002.
 - [26] Y. Wang. Vortex Rossby waves in a numerically simulated tropical cyclone. part ii: The role in tropical cyclone structure and intensity changes*. *Journal of the atmospheric sciences*, 59(7):1239–1262, 2002.
 - [27] S. Casertano. Rotation curve of the edge-on spiral galaxy NGC 5907: disc and halo masses. *Monthly Notices of the Royal Astronomical Society*, 203:735–747, 1983.
 - [28] T. S. Van Albada, J. N. Bahcall, K. Begeman, and R. Sancisi. Distribution of dark matter in the spiral galaxy NGC 3198. *The Astrophysical Journal*, 295(305-313):1–10, 1985.
 - [29] J. Kormendy. Evidence for a supermassive black hole in the nucleus of M31. *Astrophys. J.:(United States)*, 325, 1988.
 - [30] D. L. Block and R. J. Wainscoat. Morphological differences between optical and infrared images of the spiral galaxy NGC309. *Nature*,

- 353(6339):48–50, 1991.
- [31] J. N. Bregman and R. A. Pildis. X-ray-emitting gas surrounding the spiral galaxy ngc 891. *The Astrophysical Journal*, 420:570–575, 1994.
 - [32] A. Inopin. Parity doublers and topology twists in hadrons. In *AIP Conference Proceedings*, volume 1030, page 298, 2008.
 - [33] Q. H. Hu. The nature of the electron. *Arxiv preprint physics/0512265*, 2005.
 - [34] S. Todorova. About the helix structure of the Lund string. *Arxiv preprint arXiv:1101.2407*, 2011.
 - [35] S. Todorova. Study of the helix structure of QCD string. *arXiv:1204.2655v1 [hep-ph]*, 2012.
 - [36] R. M. Santilli. Isonumbers and genonumbers of dimensions 1, 2, 4, 8, their isoduals and pseudoduals, and "hidden numbers" of dimension 3, 5, 6, 7. *Algebras, Groups and Geometries*, 10:273, 1993.
 - [37] R. M. Santilli. Rendiconti circolo matematico di palermo. *Supplemento*, 42:7, 1996.
 - [38] C. X. Jiang. Fundamentals of the theory of Santillian numbers. *International Academic Presss, America-Europe-Asia*, 2002.
 - [39] R. M. Santilli. Hadronic mathematics, mechanics and chemistry. *Volume I, II, III, IV, and V, International Academic Press, New York*, 2008.
 - [40] C. Corda. Introduction to Santilli iso-numbers. In *AIP Conference Proceedings-American Institute of Physics*, volume 1479, page 1013, 2012.
 - [41] C. Corda. Introduction to Santilli iso-mathematics. In *AIP Conference Proceedings-American Institute of Physics*, 2013.
 - [42] A. E. Inopin and N. O. Schmidt. Proof of quark confinement and baryon-antibaryon duality: I: Gauge symmetry breaking in dual 4D fractional quantum Hall superfluidic space-time. *Hadronic Journal*, 35(5):469, 2012.
 - [43] N. O. Schmidt. A complex and triplex framework for encoding the Riemannian dual space-time topology equipped with order parameter fields. *Hadronic Journal*, 35(6):671, 2012.
 - [44] N. O. Schmidt and R. Katebi. Protium and antiprotium in Riemannian dual space-time. *Hadronic Journal (in press)*, 36, 2013.

- [45] N. O. Schmidt and R. Katebi. Initiating santilli's iso-mathematics to triplex numbers, fractals, and inopin's holographic ring: preliminary assessment and new lemmas. *Hadronic Journal (in press)*, 36, 2013.
- [46] S. Souma and B. K. Nikolić. Spin Hall current driven by quantum interferences in mesoscopic Rashba rings. *Physical Review Letters*, 94(10):106602, 2005.